Performance Evaluation of Styrene-butadiene-styrene (SBS) Modified Asphalt Mixtures using Dynamic Modulus Test

Muhammad Bilal

(00000274544)

A thesis submitted in partial fulfillment of

the requirements for the degree

Master of Science
in
Transportation Engineering

MILITARY COLLEGE OF ENGINEERING (MCE) RISALPUR
DEPARTMENT OF CIVIL ENGINEERING
NATIONAL UNIVERSITY OF SCIENCES AND TECHNOLOGY (NUST)
SECTOR H-12, ISLAMABAD, PAKISTAN. (2022)

THESIS ACCEPTANCE CERTIFICATE

Certified that final copy of MS thesis written by **ENGR. MUHAMMAD BILAL Reg. No. 00000274544** of **Military College of Engineering**, National University of Sciences & Technology, Risalpur Campus, has been vetted by the undersigned, found complete in all respects as per NUST Statutes / Regulations, is free of plagiarism, errors, and mistakes and is accepted as partial fulfillment for the award of **MS degree in Transportation Engineering**. It is further certified that necessary amendments, as pointed out by GEC members of the scholar have also been incorporated in the said thesis.

Signature: _____

Name of Supervisor: **Dr. Inam Ullah Khan**

Date:

Signature **(HOD)**: _____

Date:

Signature **(Dean/Principal)**: _____

Date:

Performance Evaluation of Styrene-butadiene-styrene (SBS) Modified Asphalt Mixtures using Dynamic Modulus Test

by

MUHAMMAD BILAL

(00000274544)

A Thesis

of

Master of Science

Submitted to

Department of Civil Engineering

Military College of Engineering (MCE) Risalpur

National University of Sciences and Technology (NUST)

Islamabad

In partial fulfillment of the requirements for the degree of

Master of Sciences Transportation Engineering

2022

DEDICATION

This thesis is dedicated to my beloved

TEACHERS

&

PARENTS, BROTHERS & SISTER

Who taught me the value of education and have never failed to give me financial and moral support for giving all my needs during the time I developed my system and for teaching me that even the largest task can be accomplished if it is done one step at a time. I'm deeply indebted to them for their continued support and unwavering faith in me.

ACKNOWLEDGEMENT

I am thankful to ALLAH (SWT), whose blessing helped me to complete my research.

First of all, the author would like to thank the Military College of Engineering for financing this study and the Transportation Laboratory for providing the lab space needed to carry it out.

I am greatly indebted to Dr. Inam Ullah Khan for his continued support, encouragement, and guidance extended to me during the entire course of research. It was his continuous persuasion that helped me to complete this research work.

I am extremely grateful to all my committee members Dr. Sarfraz Ahmed and Dr, Javed Iqbal for their motivation, knowledge, and guidance at every stage of the research and writing of this thesis.

I am grateful to all my coursemates, work colleagues, and friends in general for their timely, indispensable continuous help and moral support in all endeavors despite their busy schedules.

(Engr. Muhammad Bilal)

LIST OF ABBREVIATIONS

AASHTO	-	American Association of State Highway and Transportation Officials
AC	-	Asphalt Concrete
ARL	-	Attock Refinery Limited
ASTM	-	American Standard Test Method
BS	-	British Standard
|E*|	-	Dynamic Modulus
G_{mb}	-	Bulk Specific Gravity
G_{mm}	-	Maximum Specific Gravity
HMA	-	Hot Mix Asphalt
J.M.F.	-	Job Mix Formula
LVDT	-	Linear Variable Displacement Transformers
NHA	-	National Highway Authority
NMAS	-	Nominal Maximum Aggregate Size
OBC	-	Optimum Bitumen Content
P_b	-	Percent Binder
P_{be}	-	Percent of Effective Bitumen
PG	-	Performance Grade
SBS	-	Styrene Butadiene Styrene
Va	-	Air Voids
V.F.A.	-	Voids Filled with Asphalt
V.M.A.	-	Voids in Mineral Aggregate

ABSTRACT

Asphalt often has polymers added to it to enhance properties that effectively lengthen the asphalt's lifespan. Styrene-butadiene-styrene is one polymer that is often added to asphalt A common modifier with a high molecular weight polymer, styrene-butadiene-styrene (SBS), has the potential to modify asphalt binder by becoming miscible with it. Characterizing the performance of SBS modified asphalt mixes and untreated asphalt mixes was the aim of this investigation. PG 60/70 AC, NHA Class B gradation and SBS YH-791 modifier has been used in this research. The dynamic modulus |E*| test conducted through a simple performance tester (SPT), was used to look at stiffness behaviour & dynamic response and was the key component of laboratory characterization testing. (21) AC specimens (3 replicas per percentage) were fabricated using a Superpave gyratory compactor for performance testing. SBS was applied in various proportions ranging from 2 percent to 7 percent by the weight of bitumen. The SPT was used to perform the |E*| test at 4.4,21.1,37.8 & 54.4 ° C temperatures and 0.1,0.5,1,5,10 & 25 Hz frequencies. Marshall Mix Design approach was employed to find Optimum Bitumen Content (OBC), The research explored the links between dynamic modulus and mixture composition under investigation and found that temperature loading frequency and SBS significantly influenced the dynamic modulus of HMA. By creating the master curves of E*, the research also produced default dynamic modulus values for conventional mixes at different temperatures and frequencies, simplifying the use of a performance-based mechanistic-empirical structural design and analysis methodology. Further, the current research attempted to estimate the dynamic modulus of SBS-modified HMA utilising Artifical intelligence (AI) modelling using Multi Expression Programming (MEPX) and Regression modelling with validation. Results showed that SBS may be easily utilized as a modifier in bitumen since it lowered penetration and ductility values by up to 46% and 56 %, respectively, and raised softening point by 63% owing to the stiffness of the mix upon increasing SBS percentage upto 7%. A blend with 6% SBS by weight of bitumen has been shown to perform better than other mixtures. In addition, an average 2.10% times increase in dynamic modulus has been observed in comparison to a conventional mix. The phase angle initially rose with rising temperature before beginning to decline after reaching a high value at 37.8°C. The HMA mix with a 6% SBS component produces the greatest outcomes overall.

Table of Contents

LIST OF FIGURES

LIST OF TABLES

Chapter 1

INTRODUCTION

1.1 Background

Almost all the pavement in Pakistan is flexible (around 98 percent). In most applications for airport runways and roadway pavement, conventional bitumen modification has proven to provide satisfactory results. However, in recent years, the need for a better highway system in a variety of climatic settings has grown significantly due to rising traffic volume and axle weights. The two main types of distress in HMA pavements are moisture damage and irreversible deformation. The major processes of moisture degradation in bituminous pavements include loss of bitumen film cohesiveness and stiffness as well as the collapse of the adhesive connection between bitumen and aggregate. The qualities of the present bituminous material might be improved to provide the high strength and lasting mixtures needed for fast roads and airports. One way to increase bituminous mixture performance is by polymer modification, which addresses bitumen's shortcomings. Modifying bitumen binders can improve a binder's overall performance by extending the range between its high- and low-temperature grades, or it can improve a binder's performance specifically in response to a given severe-service condition, such as a pavement carrying a lot of traffic or having a lot of heavy, slow-moving vehicles. The qualities of bituminous mixes have recently been enhanced by the inclusion of several types of polymers.

When applied to roads, a polymer must correctly mix with bitumen to create a uniform mixture that increases the material's resistance to rutting, stripping, cracking, fatigue, aging, etc. The mechanical properties of bituminous mixtures, such as aging permanent deformation, low-temperature cracking, moisture damage resistance, etc. can be greatly improved using elastomers, which are among the many types of polymers that are currently available. SBS is one of the most used elastomers. An increase in penetration index after SBS addition demonstrated its role in the binder's decrease in brittleness and temperature sensitivity. The physical and cross-connecting of molecules into three-dimensional networks are the source of the strength and elasticity of SBS copolymers.

Most often, the Marshall and Haveem mixture design approaches are employed to indirectly regulate the pavement performance by regulating the HMA mixture. As a result,

it is an indirect empirical connection since these approaches largely consider phenomenological mixture features, such as stability and density/voids studies of laboratory prepared HMA mixture.

The focus on exploiting more basic mechanical qualities during the last twenty years has led to more successful attempts in this area. The initial step in that direction was the creation of Superior Performing Asphalt Pavements (Superpave), a revolutionary performance-based grading and mixture design and analysis system by the Strategic Highway Research Program (SHRP), the USA As a result, there has been a global decline in the usage of empirical mixture design techniques like Marshall and Hveem. However, in Pakistan, highway officials are still working to fully apply and employ the Superpave rules and mixture design approach.

The American Association of State Highway and Transportation Officials (AASHTO) design guides (AASHTO 1986, AASHTO 1993), which are primarily empirical, are the foundation for the structural design methods for flexible pavements that many transportation authorities around the globe already use. To direct users to the best design that keeps deformations below a threshold level, equations that simulate the pavement's reaction are produced in these empirical techniques. These methods provide estimates of pavement performance based on information from earlier field tests (such as the AASHTO road test conducted in the 1960s) and, in some instances, on experience. The limits of these methods have, however, become increasingly obvious because of the greater understanding of pavement mechanics and materials and ongoing advancement in the methods of transportation. Furthermore, it is questionable and unsatisfactory how well they can forecast how a planned structure would operate under circumstances other than those on which these empirical connections were established.

The need for a more thorough mechanistic pavement design model that could forecast the performance of proposed structures was driven by the rise in the early breakdown of asphalt pavements within a few years after installation. Various initiatives have been made over the last several decades to improve the mechanical component of the design and subsequently provide a complete substitute for the empirical method. AASHTO, in collaboration with the Federal Highway Administration (FHWA), United States, sponsored a significant effort in this area. M-EPDG was developed in 2002 with special attention paid to the implementation of mechanistic-empirical structural design practices,

which necessitate laboratory testing of commonly used materials to establish an input library for the library.

The 2002 M-EPDG may assist engineers and pavement designers to accomplish their core aim of ensuring the proper performance, and in most cases, it has Furthermore, the structural design of pavements can be achieved by iteratively adjusting layer thickness and material composition to achieve responses (stress/strain) that allow for acceptable performance at the end of a design/analysis period, by this method of construction.

M-EPDG was developed in 2002 with special attention paid to the implementation of mechanistic-empirical structural design practices, which necessitate laboratory testing of commonly used materials to establish an input library for the library.

1.2 Problem Statement

In Pakistan, highway organizations invest a significant sum each year in pavement design, construction, upkeep, and repair to provide the appropriate quality of service, prevent frequent road issues, and lessen pain while traveling. But in recent years, the early failure of both newly built and old restored roadways in form of cracking and rutting has increased. Engineers and mixed designers have a high possibility of reducing distress levels if the degree of distress can be anticipated during the design process. They may do this by simulating the effects of utilizing various kinds of materials to find the best mix of materials and structure. By using algorithms based on factors including pavement structure, climate, projected traffic loads, qualities of the materials to be utilized in the pavement, and base and sub-base properties to estimate pavement performance, the 2002 M-EPDG has made this feasible.

To use the newly established volumetric design mix and mechanistic-empirical structural design techniques, research is needed to characterize the typical HMA and SBS modified HMA mixtures. In this regard, the effect of different dosage (2%, 3%, 4%, 5%, 6% & 7%) SBS modifiers on the properties of asphalt will be compared by consistency testing (penetration, softening point & ductility) and super pave testing i.e., Dynamic Modulus (D.M. or |E*|), and Test will be carried out for characterizing the SBS Modified Asphalt.

1.3 Objectives of the Study

Characterization of frequently used materials and modifiers by laboratory experiments is required for the implementation of the mechanistic-empirical design method. In terms of the dynamic modulus values of regularly used HMA and modified HMA mixes, Pakistan presently has little to no information. The objectives of this study are:

i. To evaluate the performance of SBS modified Asphalt using consistency tests.
ii. To determine the response of HMA under repeated loading with various ratios of SBS using dynamic modulus test as compared to conventional asphalt concrete mixtures respectively.
iii. To evaluate the optimum percentage of SBS for better Pavement Performance.

1.4 Scope of the Study

In our study the effect of different dosage (2%, 3%, 4%, 5%, 6% & 7%) SBS modifiers on the properties of asphalt will be compared by consistency testing (penetration, softening point,) and super pave testing Dynamic Modulus (D.M. or |E*|), Test will be carried out for characterizing the SBS Modified Asphalt. NHA class B gradation is used for the aggregate material acquired from "Babozai Quarry" located in Katlang Tehsil of District Mardan and the binder source is Attock Refinery Limited (ARL) 60/70. The SBS modifier (Y.H. -791H) is imported from “China". Before performing performance testing on the Superpave gyratory specimens, the conventional Marshall Method was used to determine the OBC and volumetric properties. Each Mix is tested for dynamic modulus at four different temperatures (4.4, 21.1, 37.8 & 54.4) and six different frequencies i.e., 0.1, 0.5, 1, 5, 10 & 25 Hz).

Table 1.1: Experimental Matrix of Bitumen Testing

Characterization	**Gradation**	**NHA – B**
	Binder	ARL 60 / 70
Binder	Tests	Standard
	Penetration	AASHTO T 49 – 93
	Ductility	AASHTO T 51-93
	Softening Point	AASHTO T 53 – 92
	Flash & Fire Point	AASHTO T 48

Table 1.2: Performance Testing Matrix of Asphalt Concrete Mixtures

TEST	Standards	SBS %	Samples	Total
Dynamic Modulus Test	AASHTO TP62	0	3	21
		2	3	
		3	3	
		4	3	
		5	3	
		6	3	
		7	3	

Table 1.3: Characteristics of Styrene Butadiene Styrene (SBS YH-791H)

	Item	SBS (YH-791H)
SBS (YH -791H)	Structure	Linear
	Melt Flow Ratio (200°C, 5kg)	0.1g/10min
	25°C, 5% Styrene solution Viscosity	2240 mPa. S
	Styrene/Butadiene (S/B)	30/70
	Hardness	76A
	Tensile Strength	20 MPa
	Volatile %	<1.0

1.5 Thesis Organization

This study is based on experiments conducted in the lab using binder and HMA combinations that have been changed and left unaltered. A thermoplastic elastomer polymer known as SBS was added to aggregate and bitumen in the materials suggested to produce the specimens. To create the samples, the mixture components were created for ACWC before being combined and compacted using SGC. Before combining the binder and aggregate, different SBS percentages (2–7%) were added to such binder in a blending procedure by the guidelines. These samples underwent Dynamic Modulus Testing using SPT. This research consists of five chapters. The history of the issue, a quick overview of

the structural design, HMA mix design, and SBS design methodologies, the need for performance testing, and the problem description, goals, and scope of the proposed study are all covered in Chapter one. The second chapter contains background information on the usage of SBS, HMA mix, and flexible pavement design approaches, advanced modulus testing methodologies, ideas of linear viscoelasticity, and results from early studies on dynamic modulus testing and dynamic modulus prediction models. The second chapter contains background information on the usage of SBS, HMA mix, and flexible pavement design approaches, advanced modulus testing methodologies, ideas of linear viscoelasticity, and results from early studies on dynamic modulus testing and dynamic modulus prediction models. The study methodology used, asphalt mixes, testing tools, sample preparation techniques, and dynamic modulus test methodologies are all explained in the third chapter. The test results, a statistical analysis, the dynamic modulus master curves, and a critique of the dynamic modulus prediction models are all provided in the fourth chapter. A summary of the findings, conclusions, and suggestions for more research are given in the fifth chapter.

Chapter 2

LITERATURE REVIEW

2.1 General

The bituminous paving mix, Hot Mix Asphalt (HMA), is a blend of properly graded aggregates that are consistently mixed and covered with bitumen to make a road (Asphalt Institute MS-4, 1988). Aggregates and bitumen are heated before mixing to achieve fluidity in the bitumen, which is necessary for proper mixing.

Design considerations for HMA pavement structures should be like those for other engineering constructions in terms of cost and durability. Premature failure of a pavement due to poor design results in higher repair costs. The best method to avoid future repair and maintenance issues is to determine the suitable construction materials and utilize proper design criteria for flexible pavements (Asphalt Institute MS-4, 1988).

The most expensive material in HMA pavements is bitumen. To make durable and economical pavements, the bitumen should be made more durable and resistant to pavement distresses, including fatigue, rutting, stripping, etc. The bitumen can be made more durable by adding certain modifiers which enhance its properties and make it more resistant to moisture-induced damages, rutting, and other pavement distresses.

Due to temperature variations, new tire designs with high pressures, many uncontrolled axle loads, and traffic patterns, pavement structure distresses have significantly grown. Considering this, researchers have given highway degradation considerable attention as they identify the root causes of this problem. Furthermore, polymer-modified asphalt, which has gained greater attention from the pavement world in recent decades, is suggested to mitigate the impacts of contributing elements (Airey, 2002)

2.2 HMA Pavement Distresses

The Pakistan National Highway and Motorway Road network is over 260,000 kilometers long and accounts for approximately 80% of Pakistan's traffic. Approximately 2.5 trillion Pakistani rupees is the value of these assets. The irony is that the condition of this asset is constantly deteriorating because of poor pavement design, poor design mix, and vice versa.

2.2.1 Rutting

Repeated loads at high temperatures are typical distresses that cause rutting in asphalt pavements (Zhu et al., 2016).In the paving layers, Rutting is an adaptation of permanent deformation. In-wheel paths occurred because of the alliance of densification and shear deformation that appear in longitudinal depressions (Xu & Huang, 2012)

In Pakistan majority of the highways and Motorways do not show resistance to rutting in the early life of the pavement. Several hot mix asphalt factors contribute to deformation in flexible pavements, such as binder properties, gradation class (how coarse or fine), types of particles, and lastly, the amount of compaction effort applied. Furthermore, factors related to loading patterns include vehicle types, tire types and pressures, vehicle speeds, and axle loads. Environmental factors, including climate and pavement temperature, also affect the type and intensity of rutting.

2.2.1.1 Disadvantages of Rutting

Various reasons enforce the distress rutting to be considered as a phenomenon not desired in flexible pavements. It has numerous disadvantages, which affect road users as well as highway agencies. Some of these are discussed below.

- Rutting is a major contributing factor in causing hydroplaning because water accumulates in rut depressions. This accumulation of water can be dangerous in the rainy season, as it reduces the skid resistance when brakes are applied.

- Rutting is responsible for causing functional failure of pavements by reducing the driver's comfort. Driver comfort is reduced because rut depressions are not uniform throughout the length of the road. This non-uniformity in rut depressions is a major cause of driver discomfort.

- Rutting in flexible pavements is also responsible for the increase in vehicle operating costs. When a tire operates in a rutted section, there is more wear and tear of the tire. Secondly, the contact area of the tire with the pavement increases. Thus, tire friction increases, and as a result, fuel consumption increases. There is an increase in the fuel expenditure because the vehicle must make extra effort to overcome additional frictional resistance due to the rutted surface.

- Rutting also encourages the water to accumulate in the subgrade layer instead of draining out. Due to this, the base or subgrade layer becomes weak, and its load carrying capacity is reduced. The weakening of these base layers increases stress concentration on top surface layers; because of this phenomenon, early deterioration of pavement occurs.

- Rutting also causes safety concerns when vehicles travel at high-speed maneuver from one lane to the other. This observation is supported by the fact that the accident rate increases as the rut of pavement increases (Miljkovic & Radenberg, 2011)

2.2.2 Fatigue Cracking

Fatigue cracking is the most common form of bitumen cracking, which occurs because of the constant wear and tear of vehicles (Kakade et al., 2016). In HMA pavements, fatigue cracking occurs primarily because of the structure's inability to withstand repeated loads, and this is the most significant source of pavement distress (Haghshenas et al., 2019).

Fracture under a variable or repeated stress is what is meant by the term "fatigue." Due to a decrease in their tensile strength, pavements are more susceptible to cracking when they are subjected to increased loads or temperature fluctuations (Al-Khateeb & Ghuzlan, 2014). HMA fatigue cracking is related to the binder percentage and the asphalt's stiffness. The higher the asphalt percentage in a mix, the more likely it is to deform (i.e., be more flexible) instead of fracture under repetitive stress (Baladi et al., 2011).

Failure of the material at ultimate strength is normally adopted criteria for characterization of material strength, and there is another important failure induced in the materials which considered as much important as ultimate strength criteria; is the fatigue criteria. Fatigue failure can be defined as the failure of material under repeated loads. If we take a copper wire and apply repeated bending, then a point comes when the wire breaks. A gas cylinder has limited charge and discharge cycles. After that, it fails. HMA pavements behave like paper clips and gas cylinders. They can carry a load up to a certain number of repetitions, and after that, pavement begins to deteriorate.

Fatigue cracking induces tensile stresses at the bottom of asphalt layers, which causes cracks that propagates towards the surface of the HMA The growth of these cracks depends on the strain level applied by fatigue stresses at the bottom of HMA. Strain levels are dependent on many factors, including stiffness of the material, dimensions, and other

properties. HMA pavement has this healing potential up to a certain limit of strain. If the strain level falls below this limit, then damage accumulation is very minimal, and damage can be repaired by chemical healing (Carpenter et al., 2012).

2.3 Styrene Butadiene Styrene (SBS)

HMA mixes are primarily composed of several types of aggregates combined in the right sizes, as well as various asphalt binder modifiers. The Styrene Butadiene Styrene (SBS) polymer modified asphalt binders are the subject of our study. SBS block co polymers are often sold in bags in bulk as solid pellets, crumbs, or ground powder. The normal asphalt cement concentration in the HMA industry is between 3% and 7% by weight. Increasing the mixing and compact temperatures while doing laboratory work and testing may be essential since the asphalt binder should be within viscosity ranges during mixing and compaction. The SBS modifier and hot asphalt cement are blended at 350-380 F. degrees Celsius using high shear mixing equipment (177-193 C).

SBS is frequently utilized by pavement engineers and in the construction of highways. There are many advantages to adopting SBS as a thermoplastic polymer, depending on the performance and qualities that apply to asphalt mixtures. Under laboratory conditions, SBS can give acceptable stiffness in asphalt mixtures based on its optimal rate, which is typically between 3% and 6% which can also improve viscoelasticity and elongation. This is in addition to improving asphalt resistance to rutting. As a result, it may be possible to enhance adhesiveness, fatigue resistance, non-recoverable resistance, and bleeding resistance. Due to constant high loading and slow traffic movements in certain locations, it is suggested that it only be used at intersections. (Roque et al., 2005)

Polymer modifiers have complicated properties, and how they affect asphalt binders depends on a variety of variables, including the amount of polymer present, its molecular weight, chemical makeup, and its molecular structure. Other crucial factors include the origin of the original asphalt binder, the manufacturing method, the grade of the binder, how the binder and modifier react, etc. To satisfy specific needs, different elastomer and plastomer combinations may be used to provide special qualities. It should be emphasized, nonetheless, that it may be quite challenging to foretell if a given combination would be able to enhance the desired feature. When combined with asphalt binders, polymer characteristics may sometimes become lessened or even altered. Compared to the PMB in the asphalt mixture, the pure polymer modified binder often has distinct structural

characteristics. Consequently, it is essential to test the polymer-modified asphalt binder; Alternatively, it would be wiser to assess the performance of genuine HMA made with modified asphalt binder under more realistic conditions. (Brule, 1999)

According to an experimental investigation by Khodaii and Mehrara (2009), adding coarse and dense graded mixes may drastically alter mechanical characteristics, notably permanent deformation of asphalt mixtures with and without SBS-modified mixtures. Other findings suggest that doing dynamic Creep testing may reveal irrecoverable deformation and that utilizing varied SBS concentrations, coarse grade-based combinations produce less persistent deformation than dense grade-based mixtures. More particularly, it was found that 5 percent SBS content suggests a suitable impact on permanent deformation in the range of 4 percent and 6 percent SBS contents. Lower stresses, it was discovered in Creep curves, do not, however, have any consequences in the test in changed mixes.(Khodaii & Mehrara, 2009)

(Kalyoncuoglu & Tigdemir, 2011) the performance of HMA may be enhanced by using (2%, 3.5%,5% & 6%) SBS polymers. By performing wheel tracking and dynamic Creep tests under different loads and temperatures, this was empirically confirmed. Additionally, it was shown via indirect tensile testing that changed asphalt mixes had higher strengths than controlled samples. To put it another way, the tensile strength of changed mixes seems to be more resistant to tensile stresses and fatigue fractures that may result in a variety of fissures. The SBS polymer seems to enhance the mechanical qualities of asphalt when combined with additional additives.

According to Chen and Huang's (Yang et al., 2010) research, adding sulfur to SBS may improve asphalt's elastic recovery. Like how differing sulfur percentage concentrations in SBS may enhance softening point while decreasing penetration, Al-Hadidy, and Tan (Al-Hadidy & Yi-qiu, 2009) discovered a similar result: although SBS and starch (S.T.) modified mixes improved the aforementioned attributes, combining the two might avoid moisture damage and temperature impacts.

The use of polymer modifiers in Superpave mix design and evaluation procedures is anticipated to result in HMAs that are stiffer at high service temperatures to reduce rutting, more elastic at intermediate temperatures to resist fatigue cracking, and softer at low service temperature range to resist thermal cracking. (2002) Chen et al. examined the morphology of the SBS modified binders as described by the presence and concentration

of the copolymer's microstructure. The dispersed polymer particles gradually swell to form local SBS networks as the polymer content rises, greatly enhancing the asphalt binder's mechanical properties (viscosity, softening point, toughness, complex Modulus, etc). Although it was found that a continuous polymer structure starts to form at an SBS concentration of between 5 and 6 percent, the exact minimum percentage relies more on the base asphalt than it does on the polymer itself. The critical network between asphalt and polymer, which seemed to be slightly higher than the phase inversion content, is what determines the optimal SBS content. (2003) Chen et al.

Researchers utilized the Hirsch model to estimate the dynamic modulus of asphalt concrete mixes based on the law of mixtures, binder modulus, and mixture content. Studies have demonstrated that the specimen shape, nominal aggregate size, loading period, and test temperature have a substantial impact on the dynamic moduli of asphalt concrete mixtures. It has been claimed that employing stiff asphalt binders at lower binder contents and lower (3 percent) air voids levels may raise the dynamic modulus values. Although there are considerable differences between the dynamic modulus values recorded in the lab and the field, discrepancies in the observed and anticipated dynamic modulus of asphalt concrete mix are found to rise with temperature.

Investigations further reveal that when compared to temperature and frequency, the impact of air voids on the dynamic modulus was not substantial. When compared to standard asphalt concrete mixes, modification of asphalt with high boiling point petroleum and SBS polymer enhances the dynamic modulus and fatigue resistance.

When predicting how HMA would behave under loading circumstances, characterization of the phenomenon is crucial. Nowadays, adding a modifier is common since several studies have shown that using modifiers with HMA to alter its qualities works. Indian researchers conducted studies that demonstrated the dynamic mechanical behavior of asphalt mixtures that included crumb rubber and the SBS polymer. Performance testing was done on the blended products, including dynamic modulus, and static and dynamic creep tests at various temperatures. For both unmodified and modified asphalt binder mixtures, master curves were created. The creep parameters that described the persistent deformation of HMA mixtures were estimated using regression analysis. In comparison to unmodified and crumb rubber asphalt binder, this research found that the |E*| had elevated values and a lesser rate of deformation upon exposure to a higher temperature. Frequency,

temperature, and Binder were shown to have a substantial impact on the dynamic mechanical behavior of asphalt by statistical analysis, specifically the multi-level factorial analysis of variance (Anjan Kumar & Veeraragavan, 2011).

The effects of lime, styrene-butadiene-styrene and styrene-butadiene-styrene on the moisture susceptibility of asphalt concrete mixes have been studied in laboratory studies. However, only a few experimental research have been carried out to determine the impact of using lime and SBS combined on the water damage to hot mix asphalt. With this research, the effects of using lime (2 percent by weight of aggregate) and SBS (2 percent, 4 percent, and 6 percent by weight of bitumen) combined in HMA on the mechanical characteristics of hot mix asphalt, particularly moisture damage resistance, were examined. On these characteristics of mixes, the effects of SBS and lime were contrasted. Conventional tests such as penetration, softening point, and Fraass breaking point, rotational viscosity (RV), and dynamic shear rheometer (DSR) tests for binders, and indirect tensile strength, Marshall stability, and stiffness modulus tests for mixtures were used to assess the physical and mechanical properties of polymer modified binders and binder aggregate mixes (Kok & Yilmaz, 2009)

(Yu et al., 2021) performed asphalt mixture performance testing. To evaluate the UV aging time and intensity equivalent conversion effect on the performance of an asphalt mixture with an SBS modifier, thirteen asphalt Specimens were prepared and molded with an optimum dosage of 5% SBS by weight of the binder. Bending modulus, dynamic modulus, and scanning electron microscopy (SEM) experiments were performed to assess the dynamic mechanical properties and micro-structure morphological features of asphalt mortar after aging. The equivalent conversion equation was created for the effective assessment of UV intensity and aging period based on dynamic mechanical analysis (DMA). The bending modulus of SBS-modified asphalt mortar rose with increasing UV intensity and aging time, according to the findings. The storage modulus and complex modulus steadily rose with the intensity of aging, while the aging influence of loss modulus and loss factor was not noticeable. The SEM results demonstrated that damage such as wrinkles, fractures, and pits formed from the top layer to the bottom of the asphalt mortar, and it can be classified into four phases.

(Cong et al., 2016) evaluated the impacts of RAP and rejuvenating agent on the performance of recovered SBS modified asphalt. At low temperatures, anti-cracking

performance, fatigue life, moisture cracking susceptibility, and other properties were examined. It was also necessary to measure the control asphalt mixture to have a better idea of the impacts of the RAP and rejuvenating ingredients. 5% SBS modified asphalt binder and rejuvenating agent were shown to have improved moisture susceptibility, rutting resistance, dynamic modulus, low-temperature anti-cracking performance, and fatigue resistance in the asphalt mixture comprising reclaimed SBS modified asphalt. As a result, the rejuvenating agent will assist in the preparation of longer-lasting RAP-containing asphalt pavement.

(Ren et al., 2021) investigated the effects of styrene butadiene rubber (SBR), waste cooking oil (WCO), and waste engine oil (WEO) on restoring and enhancing the performance of old asphalt. Rotational viscometer (RV), dynamic shear rheometer (DSR), and bending beam rheometer (BBR) techniques were used to evaluate the rheological characteristics of old and regenerated asphalts. Also investigated were the compatibility, aging characteristics, and rejuvenation method of rejuvenated asphalts. The findings showed that WCO and WEO both improved the viscosity, fatigue resistance, and fracture resistance of asphalt that had been rejuvenated, but they had a negative impact on temperature sensitivity, rutting resistance, elastic recovery, compatibility, and aging characteristics. The temperature sensitivity, high and low-temperature performance, compatibility, and aging resistance of the revitalized asphalt were all further enhanced by the addition of SBR. In addition, WCO rejuvenated asphalt performed better in terms of fatigue cracking resistance, whereas WEO had greater rutting resistance, creep recovery, and compatibility. The ideal dose of waste oil and SBR was suggested as 10 wt percent and 3 wt percent, respectively, considering the total performance of rejuvenated asphalt.

In another research, various doses of SBS modification were applied to the SK70# and SK90# matrix asphalt (Zhang et al., 2019). The effectiveness of each SBS-modified asphalt was tested using the test procedures used in China and Superpave, from which the proper assessment index of SBS-modified asphalt was derived. According to the findings, adding an SBS modifier boosted asphalt binder viscosity at high temperatures while also lowering its temperature sensitivity and improving high-temperature performance. It was not advised to use the penetration test to gauge how well SBS-modified asphalt performed because of the unpredictability that the swelling of the asphalt caused in the test's findings. The softening point of SBS-modified asphalt rose by 5.7 percent, 12.8 percent, 22.5 percent,

and 26.4 percent, respectively, compared to matrix asphalt for SK70# matrix asphalt, and by 21.2 percent, 26.3 percent, 33.6 percent, and 46.6 percent, respectively, for SK90# matrix asphalt. When SK90# matrix asphalt is compared to SK70# compound asphalt, the influence of the SBS-modifier on the latter's softening point is considerably better. As the test temperature dropped, so did the SBS modifier's improved impact on the low-temperature performance of matrix asphalt. It is advised to conduct a BBR test when examining how the SBS modifier affects the low-temperature performance of the asphalt binder.

To prepare hot mix asphalt (HMA) containing different aggregates (marble, granite, and quartzite), (Singh et al., 2013) studied the impact of bitumen modification with varying percentages of Styrene butadiene styrene (SBS 3 percent, 5 percent, and 7 percent) and compared the results with mixes prepared with neat VG 30 HMA Based on how much silica oxide and calcium carbonate are contained in the aggregates, their acidic and basic natures have been determined. The mixing and compacting temperatures of modified bitumen and the performance grade based on the G/Sin value were calculated using a dynamic shear rheometer (DSR). Mixtures of plain bitumen aggregates and SBS-modified bitumen are compared for their physical and mechanical qualities. To assess the sensitivity to moisture, tensile strength ratio (TSR) tests and the wheel tracking test was conducted. The wheel tracking test was used to evaluate the findings of samples' permanent deformation. The findings show that the SBS modified mixes' strength properties, rutting resistance, and moisture susceptibility are significantly improved. Basic aggregates those with greater calcium (Ca) content bond with plain bitumen better than acidic aggregates, or those with higher silica (Si) content. But with modified bitumen, siliceous aggregates exhibit a greater percentage improvement in strength and moisture susceptibility than calcareous aggregates.

2.4 Dynamic Modulus $|E^*|$

The stiffness of HMA, which may partly describe its viscoelastic nature, is thought to be reflected in its dynamic modulus. It represents the absolute value of the complex modulus E* and measures how resistant the HMA is to deform under sinusoidal stress. For linear viscoelastic materials, the complex modulus (E*) is the relationship between stress and strain under continuous sinusoidal loading (Witczak et al., 2002). The real component of the complex modulus is a complex number and quantifies the inner damping or viscosity, and the imaginary component indicates the elastic stiffness (Huang, 2004). Equation 2-1

may be used to express the real and imaginary parts of the complex modulus (E*). (Witczak and others, 2002)

$$E^* = E' + iE''$$ Equation 2.1

Where:

í = √-1

E'' = loss or viscous modulus

E' = storage or elastic Modulus

Therefore, E* corresponds to the elastic component for any material with only one property: elasticity. When expressed mathematically, the dynamic modulus is equal to the product of the maximum applied stress and Elastic materials have an E'' value of 0, so the elastic component equals E*. The dynamic Modulus is defined by Equation 2.2 as the product of the maximum recoverable axial strain and dynamic pressure stress (Huang, 2004). It is important to remember that although though dynamic modulus is the complex modulus's absolute value, it is only represented by the letter E*.the peak recoverable axial strain (ε_o),

$$E^* = \frac{\sigma_o}{E_o}$$ Equation 2.2

Where:

ε_o = strain amplitude (με)

σ_o = stress amplitude (psi)

E* = dynamic modulus (psi)

Equation 2.3 illustrates the phase angle as the angle by which the imposed compressive stress (lags the produced axial strain) (Huang, 2004). Using Equations 2.3, we can express the phase angle mathematically (Witczak et al., 2002).

$$\emptyset = \frac{t_i}{t_p} \times 360$$ Equation 2.3

t_i = time lag between a cycle of stress and strain (s)

t_p = time for a stress cycle (s)

i = imaginary number

Since Ø = 0 for an entirely elastic material, the complex modulus equates to the dynamic modulus' absolute value which is 90. Equation 2.1 shows how the angular velocity, and time, t, create the sinusoidal stress and the consequent strain, implying that the phase lag expresses the time dependence of HMA Additionally, it may be said that HMA depends on the frequency of loading based on the formulae for Equation 2.1 shows the relationship between stress and resultant strain as a result of angular frequency, which is connected to the loading frequency shown in Equations 2.4 (Huang, 2004).

$$\Omega = 2\pi f \qquad \text{Equation 2.3}$$

Where:

Ω = angular frequency (rad/s) f = loading frequency (Hz)

Numerous investigations have shown that HMA is temperature dependent in addition to frequency dependent. This was shown by laboratory testing of HMA at various test temperatures, which produced varying recoverable strain magnitudes and, therefore, varying dynamic modulus.

2.5 History of Dynamic Modulus Testing

One approach to describing the stress-strain relationships of viscoelastic materials is dynamic modulus (Huang, 2004). To characterize the viscoelastic characteristics of HMA, Papazian became among the first to employ it as a test procedure. The idea is not brand-new (Papazian, 1962). The tests were carried out on cylindrical samples of HMA at various load amplitudes and frequencies in a temperature-controlled environment. At a specific loading frequency, sinusoidal stress was applied, and at that same frequency, the ensuing sinusoidal strain response was found. This research suggested using viscoelastic ideas to improve the performance and design of asphalt pavements.

Throughout the next ten years, several experiments were carried out that looked at compression, tension, and tension-compression loading and showed how varied loading circumstances affected dynamic modulus. According to some experts, higher test temperatures resulted in more obvious and significant effects (Kallas, 1970). Others argued that tension-compression loading was preferable for use in field loading circumstances because it was more precise. Additionally, they were able to anticipate the behavior of the asphalt concrete under field loading circumstances better by using a bi-modular analytic

approach that included the Modulus discovered in both tension and compression (Khattab et al., 2014)

Several further experiments were carried out in the late 1980s and early 1990s employing various specimen shapes, testing geometries, and loading circumstances in addition to the testing conditions. Due to the international testing program run by the Technical Committee on Bitumen and Asphalt Testing of the International Union of Testing and Research Laboratories for Materials and Structures (RILEM), Testing was conducted by 15 cooperating labs in locations around Europe including the complicated modulus tests. The main goal is to assess and improve different mix design approaches for asphalt pavements. The results showed that the indirect tension tests carried out under certain loading circumstances and the bending tests had an acceptable degree of agreement (Francken et al., 1996). The researchers also tried calculating the dynamic Modulus of HMA using a Superpave shear tester (SST). However, it has not been chosen as a standard test process owing to several disadvantages. The main disadvantage was the variety in the modulus values acquired by SST. under the same testing circumstances. By expanding the number of samples, using more LVDTs, and using other statistical analysis techniques, efforts were made to reduce testing variance

According to ASTM "D3497-79," HMA's dynamic Modulus may be determined using these standard test procedures provided in this document (2003). The testing of a cylindrical HMA is required by this standard. This specification calls for testing a cylindrical HMA specimen at three temperatures, namely 41, 77, and 104 ˚ F, and three frequencies, namely 1, 4, and 16 Utilizing strain sensors that are permanently adhered to the specimen's middle, the axial strain is determined after the specimen is exposed to a sinusoidal force. The dynamic modulus is then determined by dividing the axial stress by the recoverable axial strain. (ASTM, 2003).

Additionally, AASHTO has designated TP62-07 as a provisional standard for dynamic modulus (AASHTO, 2007). This technique is a frequently used lab test for |E*|. A cylindrical specimen of HMA must also be subjected to compressive axial stress, as required by ASTM. However, testing is necessary for six frequencies 0.1, 0.5, 1, 5, and 10 Hz; and five temperatures 14, 40, 70, 100, and 130°F. Linear variable differential transformers are used to calculate recoverable strain from axial deformations observed at

two, three, or four separate sites (as needed) (LVDTs). The stress-to-strain ratio, or dynamic modulus, is then computed (AASHTO, 2007).

2.6 Evaluation of Dynamic Modulus

A growing number of scientists are focusing on the Dynamic Modulus of HMA as a design input factor for the M-material EPDG's characterization of asphalt concrete and as a viable candidate to conduct an easy performance test to assist in the design of the Superpave mix. Numerous studies have been conducted in recent years to determine the factors that affect the dynamic Modulus. Temperature and load frequency are widely regarded to be the two most important parameters in influencing E*. For many years, researchers have shown that a reduction in temperature and an increase in loading frequency are both associated with an increase in dynamic Modulus. The reaction of the mix is also influenced by the qualities of the HMA components, such as aggregate and asphalt cement, in addition, to testing the temperature with loading frequency. Numerous investigations have been carried out to better understand the variables influencing |E*|.

Bonnaure and associates used a sinusoidal force on trapezoidal specimens in a bending test to ascertain the asphalt mixes' modulus. According to their findings, temperature and loading frequency both significantly impacted the stiffness of asphalt, as measured by |E*|. Furthermore, the rigidity of the mix was influenced by the volume of aggregate and the number of air spaces in the mix (Bonnaure et al., 2004).

The University of Minnesota did research that was funded by the Minnesota Department of Transportation (Mn/DOT) to measure the dynamic Modulus of common Minnesota asphalt mixes. Four distinctive mixtures with four distinct binder grades or kinds and varying specimens' preparation techniques were subjected to dynamic modulus testing. The investigation concluded that combinations with stronger binders produced greater values of |E*|. Additionally, sample preparation methods had little impact on the findings of the dynamic modulus test (Timothy et al., 2003).

Kim and colleagues utilized their dynamic modulus tests to create a database of 42 frequently used asphalt blends in North Carolina. These combinations vary from one another in terms of the sources and grades of the aggregate, the grades and sources of the asphalt, the mix design, or the amount of asphalt. The database was used to research how mixture factors affected the dynamic Modulus. According to the study's findings, aggregate

sources, and gradation under the NCDOT Superpave classification did not seem to have a substantial impact on dynamic Modulus. Furthermore, the dynamic Modulus of asphalt mixes seemed to be influenced by the source, Performance Grade (PG), and quantity of asphalt (Kim et al., 2005).

Dynamic modulus tests were done by Virginia Tech Transportation Institute on eleven distinct surfaces, intermediate, and base course mixes that were gathered from various asphalt factories around Virginia to characterize HMA in compliance with M-EPDG. In the study, it was shown that the dynamic modulus of a given mix may be affected by a variety of factors, including the kind of aggregate, the asphalt content, and the proportion of R.A.P.

With the assistance of the Oklahoma Department of Transportation, research was carried out at Oklahoma State University (OSU) to assess the variables impacting dynamic modulus and obtain a high degree of dependability for M-EPDG (ODOT). 21 distinct mixtures, each with 3 different kinds of binder and 4 different kinds of aggregates, were chosen for the investigation, and |E*| were carried out at six different loading frequencies and four different temperatures. To compute |E*| below 0°C, it was observed that testing at -10°C resulted in significant frost formation upon that frame, samples, and LVDTs. Cored test specimens with 4.5 + 1.0 percent accuracy may be produced by compressing the specimen to 6.0 + 1.0 percent. In addition, to test temperature and frequency, it has been noted that PG grade has a significant impact on |E*|. However, neither the nominal aggregate size nor the mix designation had a substantial impact (Cross et al., 2007).

According to the results of the investigations stated above, dynamic Modulus is a crucial material characteristic of HMA that more accurately captures its viscoelastic nature. Actual laboratory testing of the components of pavement is required for the deployment of M-EPDG to have the highest level of dependability. HMA must be characterized at the regional level in terms of |E*| since it is a component of pavement. which have been tried at state and regional levels in the United States. To make it easier to adopt the Mechanistic-Empirical structural design method, especially M-EPDG in Pakistan, the same must be done there for the characterization of typical HMA mixtures.

2.7 Summary

The stiffness of HMA may be partly described as viscoelastic by its dynamic modulus. When HMA is exposed to continuous sinusoidal loading, Absolute complex modulus (complex modulus ratio) is defined as the ratio of maximal dynamic stress to the highest recoverable axial strain. Dynamic Modulus' behavior is temperature and frequency-dependent, which makes it useful for describing the viscoelastic properties of HMA The dynamic HMA Modulus has been determined using a variety of test techniques. AASHTO TP 62-07, however, is the most modern and commonly utilized.

Studies revealed that temperatures and loading frequency are the key determinants of the dynamic Modulus of HMA Mix volumetric parameters, aggregate type, and aggregate interactions are other major elements that determine the dynamic Modulus of HMA, as are the nominal maximum aggregate size and the number of binders used.

The dynamic Modulus of HMA is the MEPDG's primary input parameter for determining material characterization. It has also been a leading candidate for an easy test performed to assist the Superpave volumetric mix design method. Thus, it acts as a direct connection between Superpave volumetric mixture design techniques and mechanistic-empirical structural design methods. The MEPDG provides three alternative material input hierarchies for designers to choose from by the degree of the desired design. For Level 1 to be the most trustworthy, |E*| values must be measured in a lab. Levels 2 and 3 employ the |E*| predictive equations, nevertheless. It has not yet been determined if these prediction equations apply to the local circumstances in Pakistan. The standard HMA mixes in Pakistan must likewise be described in terms of |E*| to execute Level One design there.

Chapter 3

RESEARCH AND TESTING METHODOLOGY

3.1 General

It contains the procedures required to achieve the study's goals, such as gathering necessary supplies, making specimens, conducting tests, and determining the relative relevance of different factors. SBS modified asphalt concrete specimens and a control asphalt concrete specimen were both used in this study. This chapter will provide a detailed explanation of the Marshal Mix design procedure for calculating OBC The Superpave gyratory compactor was used to produce the SBS modified specimens with percentages ranging from 2 to 7 percent after mixing the needed quantity of SBS with the binder using a high shear mixer. These laboratory specimens were prepared using the NHA-B wearing course grading method, as described in this chapter. The procedure for preparing test specimens, the laboratory tests that were to be performed on the samples, the testing apparatus that was utilized, and the test input parameters are all described in this chapter.

3.2 Research Methodology

To accomplish the objectives, the SBS modifier (YH-791H) is imported from "Shijiazhuang Tuya Technology Co. Ltd, Shijiazhuang City, China". NHA class B gradation is used for the aggregate material acquired from "Super-Babozai Quarry" located in Katlang Tehsil of District Mardan and the binder source is Attock Refinery Limited (ARL) 60/70. SBS modified Specimens for wearing course mixes were created in the laboratory under controlled circumstances. These specimens were prepared following the laboratory diagnosis of OBC and then tested for Dynamic Modulus testing. Following that, the data were analyzed and subsequent conclusions and recommendations were made. The approach for this investigation is depicted in Figure 3.1.

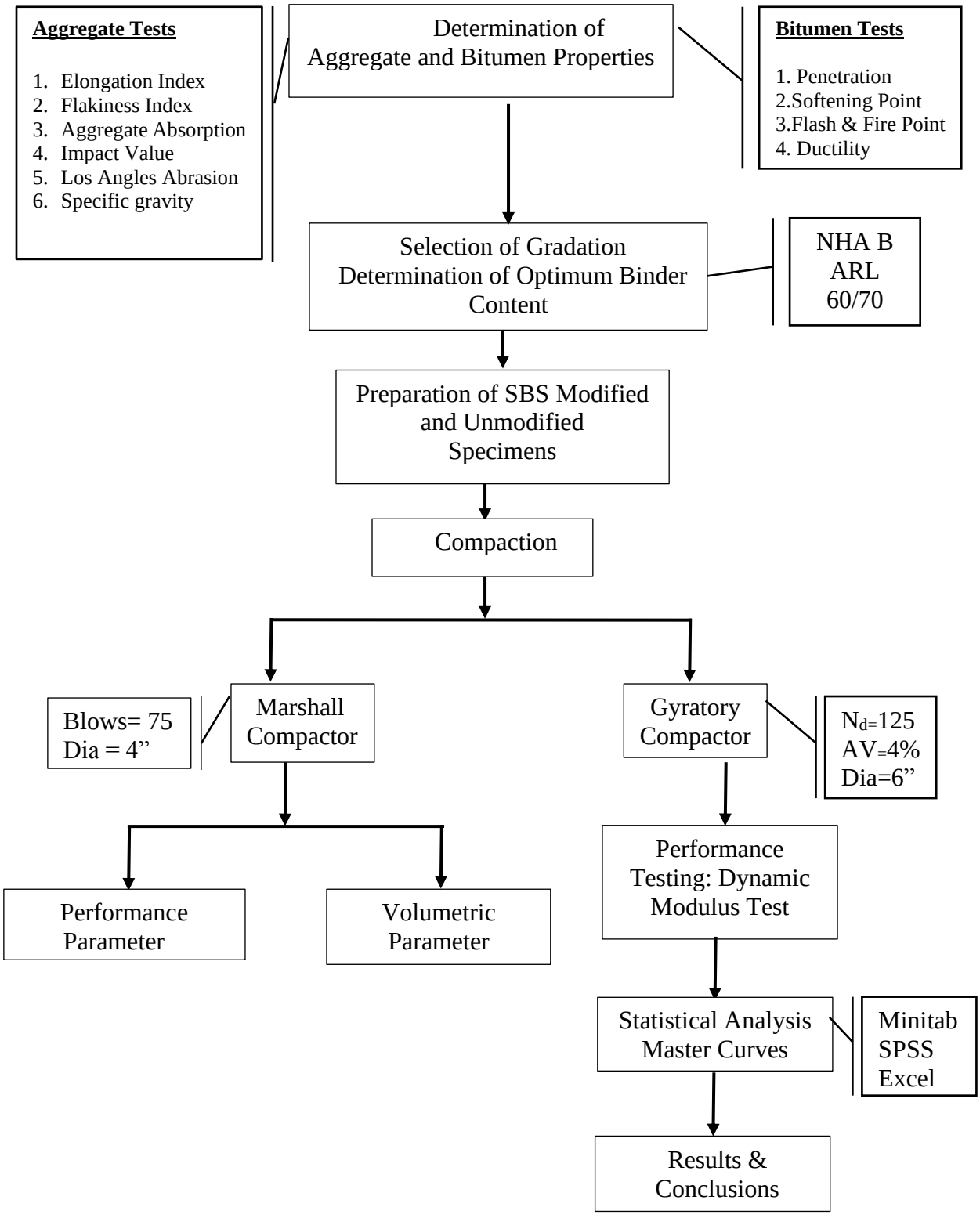

Figure 3.1: Flow Chart of Research Methodology

3.3.1 Material Selection

Babozai quarry located in Katlang Tehsil of district Mardan provided the coarse and fine aggregates, and Attock Refinery Limited (ARL) in Rawalpindi provided penetration grade 60/70 bitumen for the project. For this study, grade 60/70 was chosen since it is

mostly used in practice in Pakistan and is suited for climatic zones with a colder to the mild environment and it is also fulfilling the criteria of NHA specifications i.e if the Mean Annual Air temperature is between 7-24C then AC 60/70 must be used. Moreover, Selected Aggregates and Binder have been also used in "The Periodic Maintenance Project (Functional & Structural Overlay) at Peshawar-Islamabad Motorway (M-1) under the supervision of NHA SBS modifier (YH-791H) is imported from "Shijiazhuang Tuya Technology Co. Ltd, Shijiazhuang City, China".

About 95% of the mix's susceptibility to permanent deformation comes from the aggregate structure, with the remaining 5% coming from the asphalt binder. Aggregates build a durable stone framework that can survive repeated load applications. The features of HMA are significantly influenced by the gradation, surface roughness, and shape of the aggregates. Compared to spherical and smooth-textured aggregates, angled aggregates have greater shear strength. According to ASTM and BS standards and regulations for material characterization, mandatory tests on utilized aggregates and asphalt binder were carried out.

Figure 3.2:Styrene Butadiene Styrene (SBS)

3.3.2 Aggregate Testing

The primary element of the mix that resists permanent deformation and is predicted to provide a sturdy structure for withstanding repeated loads is the aggregate arrangement. Aggregate samples were taken from each stockpile and analyzed in a laboratory to determine their gradation and density. The following laboratory tests are included:

- Los Angeles Abrasion Test on aggregate
- Aggregate Crushing Value Test
- Aggregate Shape Test
- Specific Gravity and Water Absorption Test aggregates
- Aggregate Impact Value Test

The tests mentioned above were carried out using three samples and the average was taken.

3.3.2.1 Aggregate Shape Test

The shape of the particles has a significant impact on the strength and workability of an asphalt mixture. It also affects the amount of work necessary for compaction, which is essential to get the right density. A shape test was used to determine how many aggregate particles were elongated and flat. According to ASTM D4791, aggregate particles are categorized as flaky or elongated depending on whether their dimension is less than 0.6 of their mean sieve size or more than 1.8 of their mean sieve size, as shown in Table 3.1.

3.3.2.2 Specific Gravity of Aggregates

The specific gravity of aggregate material is a measure of its weight-to-volume ratio. Gravities of several types of aggregate were measured, including coarse, fine, and filler. Granular material that passes through a No. 4 sieve is referred to as coarse granular material.

3.3.2.2.1 Specific Gravity of Coarse Aggregates

The ASTM C 127 methodologies and instruments were used to determine the coarse aggregate's specific gravity and water absorption. There are three sample conditions for the coarse aggregate specific gravity test: oven-dry without water in the sample, immersed in water or underwater and saturated dry on the surface. The test was completed on both the 10-20 mm and 5-10 mm coarse-graded stockpiles, with the results reported in Table 3.1.

3.3.2.2.2 Specific Gravity of Fine Aggregates

In line with ASTM C 128 techniques and equipment, the specific gravity of fine aggregate and the water absorption of fine aggregate was determined. For fine aggregate and stone dust, a specific gravity test was carried out to determine the bulk, specific surface density (SSD), and apparent specific gravities, with the findings shown in Table 3.1.

Figure 3.3: Fine Aggregate Specific Gravity Apparatus

3.3.2.3 Impact Value Test

An aggregate's resilience to a sudden shock is shown by its aggregate impact value. The tools required to calculate the impact value include impact testing equipment, a tamping rod, and sieves in the sizes of 1/2", 3/8", and #8. (2.36mm.) 350g of aggregate that passed through a 1/2" sieve but was still on a 3/8" sieve was gathered, layered in three layers, and tamped 25 times in the mold of the impact testing machine. A hammer weighing 13.5 to 14 kg was used to strike the sample 15 times from a height of 38 cm after it had been transported to the machine's larger mold. The resulting aggregate was taken out and sifted using sieve #8. The impact value was calculated using the percentage of aggregate that passed through a 2.36mm sieve.

Figure 3.4: Impact Value of Aggregate Apparatus

3.3.2.4 Crushing Value Test

The aggregates must be able to bear traffic loads to produce pavement of greater quality and strength. A steel cylinder with open ends, a base plate, a plunger with a 150 mm piston diameter, and a hole in the centre for inserting a lifting rod, a cylindrical measure, a balance, a tamping rod, and a compressive testing machine made up the test equipment. The selected aggregates were those that made it through a set of sieves measuring 12" and kept on 3/8". The aggregate sample was cleaned, oven dried, weighed (W1), and then layered onto the cylindrical measure in three layers with 25 tamps between each layer. The sample was put inside the steel cylinder that had three base plate layers. Once the total load reached 40 tonnes, it was then placed into compression testing equipment at a rate of 4 tonnes per minute. The crushed material was then passed through a 2.36mm filter after the steel cylinder was removed. The materials that passed through this filter were gathered and weighed (W2). The formula =, W-2/W-1*100 was used to calculate the crushing value of aggregate.

Figure 3.5: Aggregate Crushing Value Apparatus

3.3.2.4 Los Angeles Abrasion Test

The abrasion resistance of the road aggregate is evaluated using this test. To survive wear brought on by heavy traffic loads, aggregate must be sufficiently resilient. A balance, a set of sieves, steel balls, and a Los Angeles abrasion machine were used in this test. This procedure made use of grade B testing. In the Los Angeles abrasion machine, 2500 g of aggregate retained on 12" and 3/8" sieves, for a total of 5000 g (W-1.) of aggregate, were

added together with 11 steel balls or charges. The machine was spun for 500 revolutions at a speed of up to 33 but more than 30 revolutions per minute. A 1.7mm sieve was then used to sift the material. The sample's weight (W2) after passing through it was noted. The following formula was used to obtain the abrasion value: W-2/W-1 100.

As a result, it's crucial to check aggregate suitability against ASTM and BS standards and material characterization criteria while creating asphalt mixtures. The aggregate from the Margalla quarry served as the subject of these tests, and the findings are summarised in Table 3.1.

Figure 3.6: Los Angeles Abrasion Value of Aggregate Apparatus

Table 3.1: Properties of Aggregate

Test Description	Specification Reference		Result	Limits
Elongation Index (EI)	ASTM D 4791		3.2%	≤ 15%
Flakiness Index (FI)	ASTM D 4791		10.6%	≤ 15%
Aggregate Absorption	Fine	ASTM C 127	2.28%	≤ 3%
	Coarse		0.61%	≤ 3%
Impact Value	BS 812		15.12 %	≤ 30%
Los Angles Abrasion	ASTM C 131		21.15%	<30%
Specific Gravity	Fine	ASTMC128	2.55	-
	Coarse	ASTM 127	2.63	-

3.3.3 Asphalt Binder Testing

Consistency, safety, and cleanliness are the three key characteristics of a binder in infrastructure and engineering applications, according to the Asphalt Institute's MS-4

manual. As a temperature, asphalt binder density fluctuates. Because of this, it is necessary to compare asphalt binder consistencies at a constant temperature. The consistency of the bitumen binder is usually assessed using a penetration test or a viscosity test. Additional information and assurance in the consistency are provided by additional tests, such as those that measure the softening point and ductility of the binder. Therefore, the following laboratory tests have been conducted to characterize the asphalt binder.

- Penetration Test
- Softening Point Test
- Flash and Fire Point Test
- Ductility of Bitumen

3.3.3.1 PENETRATION TEST

The penetration of asphaltic substances may be evaluated via penetration testing. In the penetration test, containers with needles and samples are utilized. With a softer binder, penetration values are improved. Unless otherwise stated, the test was conducted by AASHTO T 49-03, with the temperature used being 25°C, the load being 100 grams, and the test lasting 5 seconds. Following penetration testing, five values were gathered from each of the two ARL 60/70 samples. The data gathered all satisfied the specifications set out by the penetration test. The outcome of the penetration test is shown in Table 3.2.

Figure 3.7: Bitumen Penetration Apparatus

3.3.3.2 Softening Point Test

Although bitumen is a viscoelastic substance, it softens and loses viscosity as the temperature rises, suggesting that it is softening. The bitumen's softening point is the

temperature at which a standard-sized sample of bitumen cannot support the weight of a 3.5-gram steel ball and is determined by a series of experiments. This implies that the bitumen softening point is often calculated as the temperature at which the bitumen softens just sufficient to enable the steel balls to drop 25 millimetres. The AASHTO T-53 requirements for assessing the asphalt softening point were observed to be satisfied using ring and ball equipment. the softening point test's findings are presented in the following Table 3.2.

Figure 3.8: Ring and Ball Apparatus

3.3.3.3 Fire and Flash Point

D3143/D3143M-13 standards were used to identify this characteristic. The accuracy of the test relies on the pace of temperature rises. Since bitumen is a liquid at high temperatures, it might catch fire. When the temperature comes close to the bitumen's flash point, it will briefly catch fire; this is the bitumen's flash point. When it stays on fire for at least five seconds, it is the bitumen's fire point. The Flash and Fire point test results are shown.in the following Table 3.2.

3.3.3.4 Ductility Test

Using ASTM -D-113-86 standards, this attribute was discovered. When two ends of a briquette specimen of the material in the shape given are dragged apart at a certain speed and temperature, it is measured by the length it will extend before breaking. The test was conducted at a speed of 5 C/minute at a temperature of 25°C.When two ends of a briquette specimen of the material in the shape given are dragged apart at a certain speed

and temperature, it is measured by the length it will extend before breaking. The test's findings for ductility are presented in the following Table 3.2.

Table 3.2: Laboratory Tests Results Performed on unmodified and SBS Modified Bitumen

Test Description	Specification	Result						
		0% SBS	2% SBS	3% SBS	4% SBS	5% SBS	6% SBS	7% SBS
Penetration (mm)	ASTM D 5-97	66	63	55	51	49	46	45
Flash Point (ºC)	ASTM D 92	252	265	274	279	287	290	294
Fire Point (ºC)	ASTM D 92	282	288	292	296	301	305	309
Softening Point(ºC)	ASTMD36-06	49	50.9	55.3	62	71.3	77.5	80
Ductility (cm)	ASTM D 113	100	97	90	81	73	66	64

3.4 Gradation Selection

NHA class B aggregates were utilized by NHA (1998) standards for dense graded surface course mixes. According to Marshall Mix Design, the nominal maximum aggregate size for class B wearing coarse gradation was 19 mm, with the actual maximum aggregate size being somewhat smaller. Table 3.3 contains the selected gradation, and Figure 3.9 depicts the gradation plotted against % passing and sieve diameters.

Table 3.3: NHA Class B Gradation Selected for Testing

Sieve Size	NHA Specification Range (%Passing)	Our Selection	Retained
19	100	100	0.00
12.5	75-90	82.5	17.5
9.5	60-80	70	12.5
4.75	40-60	50	20
2.38	20-40	30	20
1.18	5-15	10	20
0.075	3-8	5.5	4.5
Pan	. . .	. . .	5.5

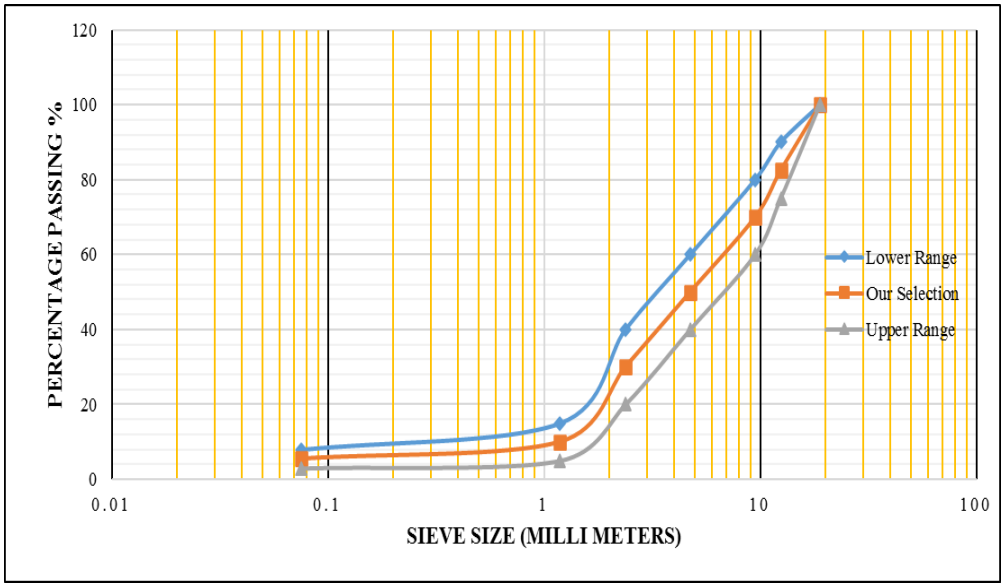

Figure 3.9 NHA B Gradation Plot

3.5 Asphalt Mixture Preparation

Laboratory-produced mixes were developed using the Marshal Mix design process after determining the OBC Following that, samples were prepared according to their OBC using especially 4% air voids. The following heading describes the method for preparing laboratory-produced mixtures.

3.5.1 Preparation of Bitumen Mixes for Marshall Mix Design

The bituminous mixes used to calculate OBC were made using the Marshall Apparatus by ASTM D 6926. The Marshall Mix design criteria were verified, the volumetric properties, stability, and flow were assessed, and then the OBC was computed. The following process led to the creation of Marshall Mix:

3.5.2 Aggregate and Bitumen Preparation for Mixes

The aggregates were dried at 105°C to 110°C after sieve testing to retain a constant weight. When using the Marshall Mix design technique, 1200 grams of aggregate are needed to compress a 4-inch diameter sample (ASTM D6926).

3.5.3 Mixing of Aggregates and Asphalt Cement

As per the ASTM D6926 standard, bitumen and aggregates should be thoroughly blended using a mechanical mixer. The dehydrated, warmed aggregates, together with the warmed bitumen, were immediately moved to the automated mixing apparatus after being removed from the oven. Figures 3.10 display the schematic representation of a mechanical

mixing apparatus. The temperature range used for mixing was 160°C to 165°C, matching Pakistan's manufacturing temperature for bituminous mixtures (NHA Specifications).

Figure 3.10: Asphalt and Aggregate Mixer

3.5.4 Compaction of Specimens

The mixes were compacted using a Marshall Compactor after being preconditioned at 135 degrees Celsius for two hours. The mould cylinder, base plate, and extension collar are the three elements that make up each part of the mould arrangement. The mould cylinder has an inner diameter of around 4 inches and a height of roughly 3 inches. You may change out the base plate and collar extensions at either the beginning or the end of the mould. Using a spatula, the mixture was squeezed into the mould. Filtering paper with a diameter equal to the mould's diameter was placed at the bottom of the mould during cleaning and preheating at 135°C before packing. when a whole batch was shoved into the mould and consistently spaded. It was covered with a layer of filter paper to shield it from the weather.

According to the findings of the previous research, the design requirement for this study was a widely used pavement or designs with ESALs (millions) 30 for dense graded wearing courses. As a result, 75 strikes were given to each end to mimic an overwhelming amount of traffic. To prepare for compression, the mould's components were inserted into the mould's holding stage (application of blows). The specimens were mechanically struck 75 times with a hammer that was properly positioned above the mould assembly. The mould assembly was removed from its holder and the specimen was rotated as soon as all the

compressive blows on one side were finished. After that, the mould assembly was put back together, and the specimen received uncompressed blows to the opposite face.

3.5.5 Extraction of Specimens from Mould

After compression, the sample was allowed to cool for a short while before the mould equipment was removed. An extraction jack was then used to remove the specimen from the mould. The prepared samples were cooled to room temperature on a flat surface. After compression, the sample was allowed to cool for a short while before the mould equipment was removed. An extraction jack was then used to remove the specimen from the mould. On a flat surface, the produced specimens were cooled down to room temperature.

3.5.6 Specimens Selection for JMF

Three specimens were created for each percent of aggregate and asphalt binder. Five different binder chemicals were used to make the specimens (3.5, 4.0, 4.5, 5.0, and 5.5 percent). Five experimental mixes were used to find the mixture that performs better at a minimal bitumen concentration of 4 percent air voids.

3.6 Volumetric Characteristics, Stability & Flow Determination

The volumetric characteristics of the mixes, such as the Voids in Mineral Aggregates (VMA) Loading continued slowly at a rate of 5 mm/minute up to failure. Marshall stability was calculated using the whole load capacity in K.N. A flow number in millimetres representing the overall deformation that takes place under the maximum load was determined. the flow number must be between 2 and 3.5, as per the Marshall Mix design criteria (MS-2). When the specimen was removed from the water bath, it was immediately analyzed. the Voids Filled with Asphalt (VFA) and the Air Voids (Va) as well as their unit weight, could be determined using the specific gravity formulae (Gmb). We were able to achieve theoretical maximum specific gravity (Gmm) and bulk specific gravity (Gmb). The Marshall Mix design criteria are more specifically shown in Table 3.3. For bituminous pavement mixes Gmm and Gmb values were calculated in line with ASTM D2041 and ASTM D2726 standards.

Loading continued at a constant rate of 5 mm/minute till failure. Marshall's stability was determined using the entire load capacity in KN. As a flow number in millimetres, the total deformation under the greatest load was determined. For a heavily travelled and worn

course, the specimen's stability must be more than 8.006 KN, according to the Marshall Mix design criteria (MS-2), and the flow number must be between 2 and 3.5. The specimen was promptly tested after being removed from the water bath.

Table 3.4: Volumetric Properties of Asphalt

% AC	G_{mb}	G_{mm}	Unit wt (g/cm^3)	V_a (%)	VMA (%)	VFA (%)	Stability (KN)	Flow (mm)
3.5	2.328	2.467	2.328	5.63	15.47	63.57	14.39	1.98
4	2.355	2.460	2.355	4.27	14.49	70.53	15.43	2.43
4.5	2.361	2.448	2.361	3.55	14.27	75.09	15.21	3.02
5	2.347	2.427	2.347	3.30	14.78	77.69	14.12	3.42
5.5	2.342	2.41	2.342	2.82	14.96	81.14	13.19	4.04

To determine the OBC of a mix the curves linking asphalt content and volumetric characteristics, stability, and flow were drawn according to the Asphalt Institute Manual MS-2 handbook.

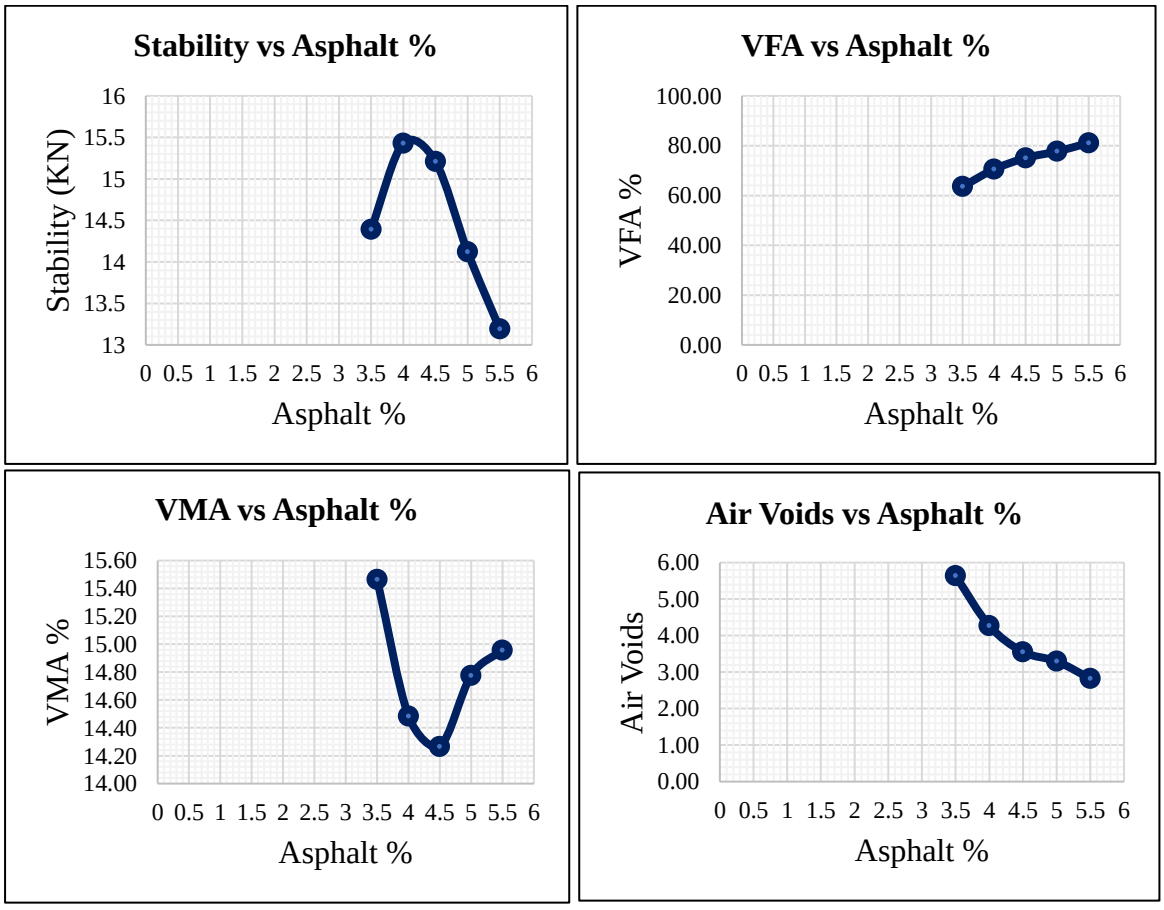

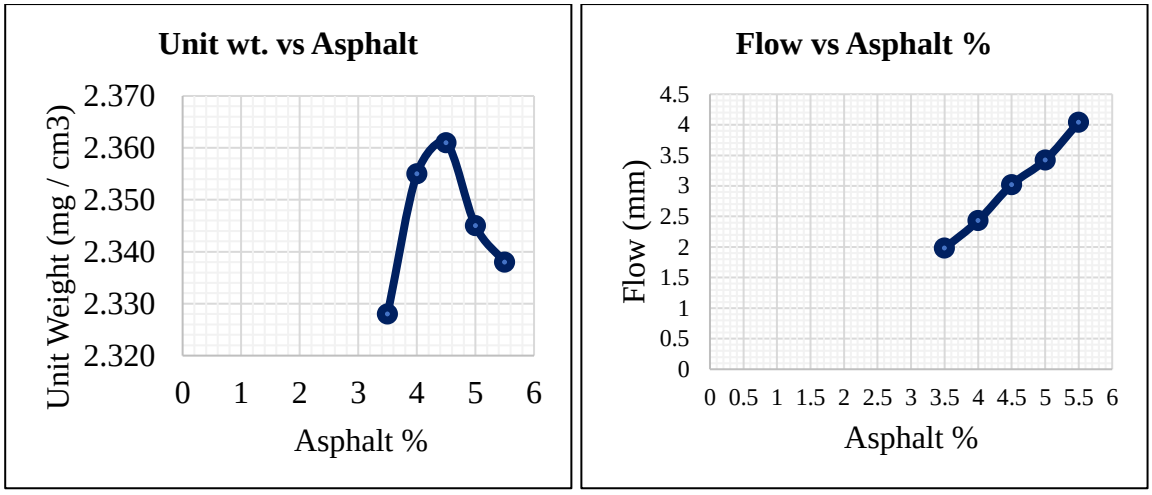

Figure 3.11: Volumetric Properties of Asphalt

Table 3.5 shows that OBC refers to asphalt with a 4 percent air void content which is 4.15 say 4.2 in our research. The plots were then used to estimate the volumetric properties, stability, and flow parameters needed by OBC. The Job Mix Formula is shown in Table 3.4, and it is evident from this that all volumetric properties, stability, and flow meet the required criteria. The VMA must not be less than 13 percent at 4 percent specified air voids, and in this instance, it was 14.35 percent. Its estimated value of 72 percent fits within the range of VFA., which should be between 65 and 75 percent. The stability value, which in this instance was 15.50 KN, was required to be more than 8.006 KN. 2.50 mm has been measured as the flow number, which is within the permissible range.

Table 3.5: Volumetric Properties of Mix at Optimum Binder Content

Marshall Parameters	Measured Value	Criteria	Remarks
OBC (%)	4.15 say 4.2	At 4% Air Voids	-------
Unit weight (g/cm^3)	2.358	N/A	-------
VMA (%)	14.35	13 (Min)	Pass
VFA (%)	72	65-75	Pass
Stability (KN)	15.50	8.006 (Min)	Pass
Flow (mm)	2.5	2-3.5	Pass

3.7 Specimen Preparation for Dynamic Modulus Testing

Marshall Mix Design method is used to find OBC Samples were prepared with 4.2% OBC by using a Superpave gyratory compactor by ASTM D 3496-99. Three Replica of

each percentage were prepared. The Bitumen and aggregate are heated upto 180°C then SBS at the rate of 500g/min were added and mixed through the high shear mixture at 500rpm initially for 30 minutes and after that, the mix will be blended for 2 hours at a speed greater than 1500rpm. The temperature should be maintained at 180°C during the whole mixing process and after proper uniform mixing the modified bitumen was kept in the oven for 2 hours to retain the obtained morphology. The mixing assembly with high shear mixer is shown in figure 3.12.

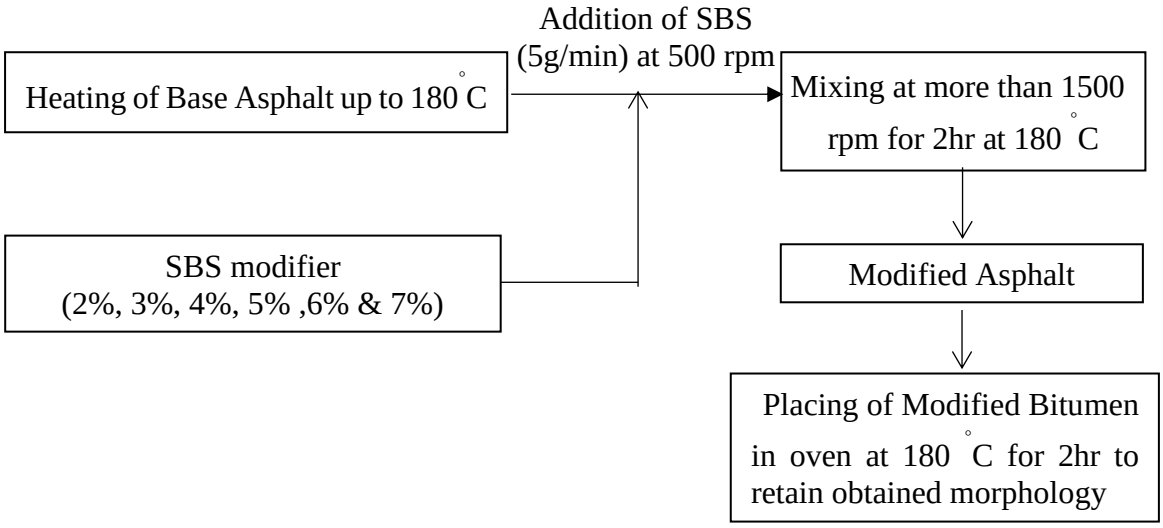

Figure 3.12: Mixing of SBS into Binder with High Shear Mixture

After blending of SBS and Binder, the SBS modified Bitumen is then mixed with aggregates using mechanical mixtures at a designed mixing temperature of 163°C to minimize segregation the samples were then compacted using SGC with dia of 150mm and

height of 170mm. To meet the AASHTO TP 62-07 standards for dynamic modulus test sample preparation, a saw cutter was used to trim the specimen height to 150mm before a 100mm dia core was taken from the center of mass of a 150mm compacted core. Fig 3.13 is showing the Gyratory sample produced by SGC and Cored samples with dia 4".

Figure 3.13: Sample Produced from SGC and Cored Samples

Make that samples are crushed to the specified air void level with a limit of less than 0.5 percent. Twenty-one (21) samples altogether, made up of three replica samples for each combination, were created using SGC, and 5-minute epoxy glues were used to install gauge points (studs) after samples had been made to the required size to measure longitudinal deformation/strain during in the testing that used a linearly variable differential transformer (LVDT). Using a gauge point fixing jig, these studs were attached to the specimen as shown in figure 3.14. Following the removal of each specimen from the assembly and securing it with the clamps that were intended to accept the LVDTs for assessing deformation, the pressure was exerted for 30 to 45 minutes on the studs to ensure that they were firmly attached.

Figure 3.14: Samples Stacked in Lab for Testing and Gauge Point Fixing Jig

3.8 Laboratory Testing

AASHTO TP 62-07 was followed in the preparation of the specimens for the Dynamic Modulus testing as the temperature rises and the frequency of loading decreases, a bitumen sample is exposed to axial compression stress that is sinusoidal (haversine). It is necessary to make use of equipment known as "Simple Performance Tester (SPT)." Compressive stress is applied, and the dynamic modulus and phase angle are produced by the stress-to-axial recoverable strain ratio.

3.8.1 Testing Equipment and Procedure

The Simple Performance Tester (SPT) utilized in this research, commonly referred to as the Asphalt Mix Performance Tester (AMPT), is a product of the IPC Global Simple firm. There are many components in the device, including an environmental chamber with an enclosed system, a data gathering system, and a heat exchanger. It was developed under NCHRP 9-19 and 9-29. It is linked to a computer system that does dynamic modulus testing using the software.

Figure 3.15: Simple Performance Tester (SPT)

Specimens are prepared before being clamped at three sites 120 apart and put in an environmental chamber with a triaxial cell and connected LVDTs. The environmental chamber has been shut, and the specimen is allowed to acclimate to the designated test temperature. AASHTO TP 62-07's recommendations for the minimum equilibrium temperature are shown in Table 3.6.

Table 3.6:Equilibrium Times (adopted from AASHTO, 2007)

Sample Temperature, °C (°F)	**Time from Room Temperature, hrs 25 °C (°F)**	**Time from Previous Test Temperature, hr**
-10 (14)	Overnight	Overnight
4 (40)	Overnight	4 hrs or overnight
21 (70)	1	3
37 (100)	2	2
54 (130)	3	1

Utilizing U.T.S. 6 software for the dynamic modulus test, the test was begun after reaching the requisite equilibrium time and the appropriate temperature. Before commencing the test, the required test frequencies were selected from the choices accessible in the program as 25, 10, 5, 1, 0.5, and 0.1 Hz. The initial dynamic modulus value required by the program is obtained via the "tuning option," which involves applying a haversine load for nine cycles. The test begins at a higher frequency, or 25 Hz, and goes down to 0.1 Hz. The program produces an output when the test is finished that includes

"Dynamic Modulus" and "Phase angle" w.r.t. a specified temperature and frequency. The U.T.S. 6 software's general user interface is shown in Figure 3-23, which was created automatically after the test was over.

In order to execute the "dynamic modulus" test on Triplicate specimens made up of 0%, 2%, 3%, 4%, 5%, 6%, and 7% SBS at four different temperatures 4.4, 21.1, 37.8, and 54.4 °C the same technique is repeated. Due to equipment limitations, the test could only be carried out at 4 C, not at -10 C. The construction of master curves is then based on the test results of the dynamic Modulus for the given temperatures.

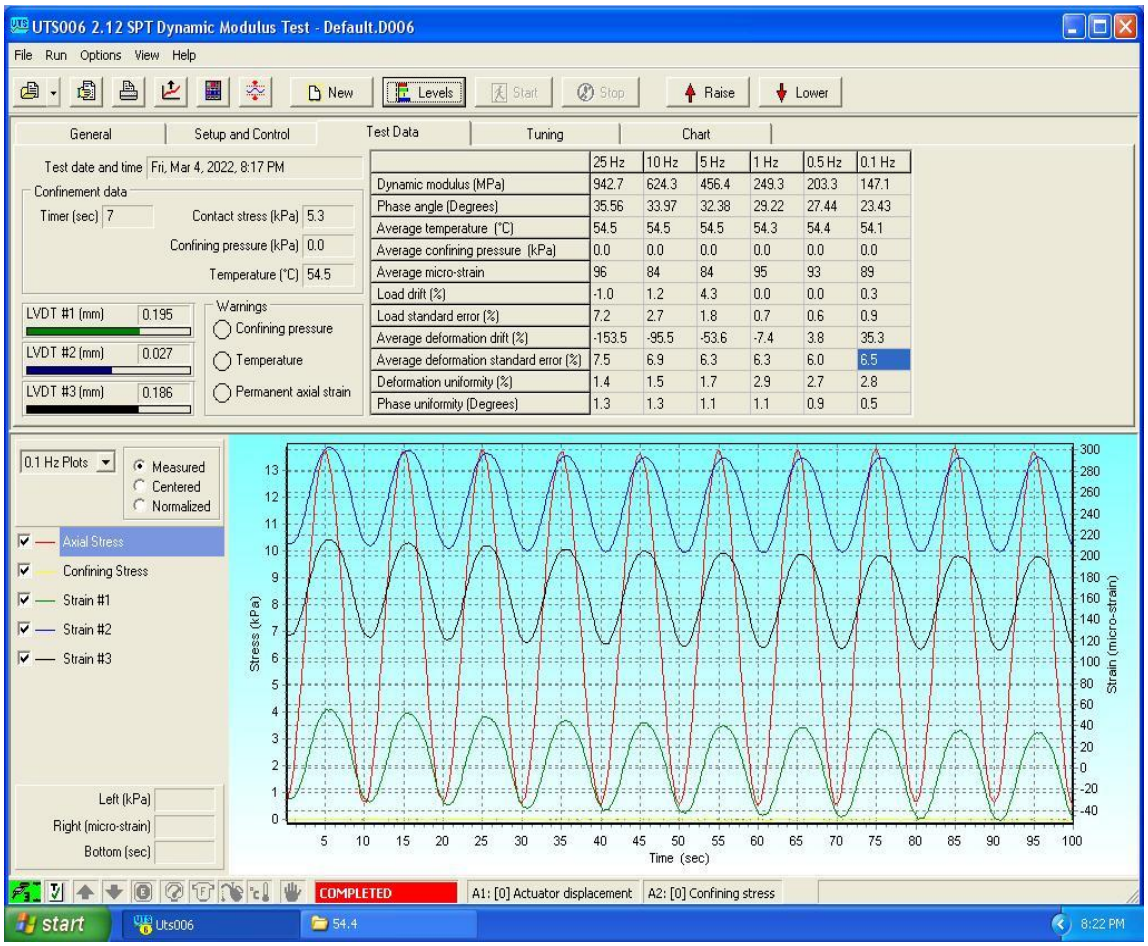

	25 Hz	10 Hz	5 Hz	1 Hz	0.5 Hz	0.1 Hz
Dynamic modulus (MPa)	942.7	624.3	456.4	249.3	203.3	147.1
Phase angle (Degrees)	35.56	33.97	32.38	29.22	27.44	23.43
Average temperature (°C)	54.5	54.5	54.5	54.3	54.4	54.1
Average confining pressure (kPa)	0.0	0.0	0.0	0.0	0.0	0.0
Average micro-strain	96	84	84	95	93	89
Load drift (%)	-1.0	1.2	4.3	0.0	0.0	0.3
Load standard error (%)	7.2	2.7	1.8	0.7	0.6	0.9
Average deformation drift (%)	-153.5	-95.5	-53.6	-7.4	3.8	35.3
Average deformation standard error (%)	7.5	6.9	6.3	6.3	6.0	6.5
Deformation uniformity (%)	1.4	1.5	1.7	2.9	2.7	2.8
Phase uniformity (Degrees)	1.3	1.3	1.1	1.1	0.9	0.5

Figure 3.16: SPT Output General Interface

3.8.2 Master Curve Development

|E*| curves in the MEPDG were utilized to identify the asphalt mixes employed in this investigation. The theory, which is based on time-temperature superposition, states that dynamic the decreased frequency, which depends on temperature and frequency, is the only factor on which modulus depends. Therefore, testing at various frequencies may be used to determine the impact of temperature variation on |E*|. Time-temperature superposition and

the "Master Curve" combine to produce |E*| values that vary in frequency and temperature. Time-temperature superposition and the "Master Curve" combine to produce |E*| values that vary in frequency and temperature. Typically, this curve formed at a temperature of 21°C. Once the reference temperature has been determined, the data at various temperatures are adjusted about the loading frequency until the curve unifies into a single smooth function. Master curve and shift factors are necessary to explain temperature and rate effects. Temperature-dependent material may be described by the master curve's frequency dependence, and the degree of shifting necessary for each temperature to produce it determines its temperature dependence.

For each combination, master curves were produced using the time-temperature superposition technique at a temperature of 21.1 °C. The master curves were constructed using an expedited technique established in phase IV of NCHRP Project 9-29, keeping in mind the testing constraints and SPT.'s inability to perform tests at -10 C. (Bonaquist, 2008). Three temperatures and four loading frequencies must be tested for this method. The master curve parameters are then determined by fitting the data to Equation 3-1.

$$Log\ |\mathrm{E}^* = \log(Min) + \frac{(\log(Max) - \log(Min))}{(1+e)\ (\beta+\gamma)\ (log\omega_r)} \qquad \text{Equation 3.1}$$

Where:

$|E^*|$ = dynamic Modulus

ω_r = reduced frequency, Hz

β, and γ = fitting parameters

Max = Maximum limiting modulus, ksi

Min = Minimum limiting modulus, ksi

Equation 3-2 uses the Arrhenius equation to get the lower frequency that is needed by Equation 3-1.

$$log\omega_r = log\omega + \frac{\Delta E_a}{19.14714} + \frac{1}{T} - \frac{1}{T_r} \qquad \text{Equation 3.2}$$

Where:

T = test temperature, °K

ω_r = reduced frequency at the reference temperature

ΔE_a = activation energy (treated as a fitting parameter)

ω = loading frequency at the test temperature

T_r = reference temperature, °K

3.9 Summary

This Section discusses in depth the study approach that was used, and a flowchart is included. In our study, NHA Class B Gradation is used. The "Babozai Quarry of Katlang Tehsil of District Mardan" provided the aggregate.PG 60/70 Binder was purchased from "Attock Oil Refinery." Furthermore, the "Structural & Functional Overlay Project at M-1" also employed the same asphalt and aggregate which are used in this study. The modifier for SBS (YH-791) was imported from China.

Through consistency testing (softening point, ductility, penetration, and flash fire point) and the dynamic modulus test, the performance of SBS modified and virgin asphalt has been compared in this study. Bitumen and SBS are combined using a high-shear mixer. According to AASHTO TP 62-07, the combined binder and aggregates were blended, and SGC was used to create the samples.

These specimens were taken from the SGC, but since they were larger than needed, they were cored and cut to create a cylindrical specimen with a 150mm height and 100mm diameter. SPT of SBS modified and unmodified samples were used in a dynamic modulus test at four different temperatures (4.4, 21.1, 37.8, and 54.4 C) and six different frequencies (25, 10, 5, 1, 0.5, and 0.1 Hz). SPT. cannot conduct tests below 4.4 °C, hence a test at -10 °C was not possible.

Additionally, this chapter discusses the requirements for testing, specimen preparation, and conditioning. Every temperature's test date was changed to coincide with a 21.1° C reference temperature and master curves were created for each sample tested for the assessment. The MS Excel solver add-in was used to create these master curves, which minimize the sum of squared errors to produce a single smooth curve for the research. Hirsch's model was used to determine the upper asymptote for the curves, or the limiting maximum modulus, and the dynamic modulus value, as measured at 37.8°C and 0.01 Hz, was used to get the lower asymptote.

Chapter 4

TEST, ANALYSIS RESULTS AND DISCUSSION

4.1 General

This section mainly discusses Phase angle and Dynamic Modulus experimental test results based on obtained results, and statistical analysis is discussed in this chapter. Consistency testing (Softening point, Ductility, and Penetration) of SBS modified, and unmodified samples are discussed. Several factors like temperature and loading frequency which affect dynamic Modulus are discussed. For each mix, Master Curve has been developed. There is also a discussion of statistical analysis, such as interaction plots and regression analyses, complete factorial designs, and analyses of variance (ANOVA).

4.2 Consistency Testing

4.2.1 Softening Point

"Softening Point" is used to assess how well the asphalt binder performs at high temperatures. The temperature at which asphalt physically changes from a viscid plastic to a viscous flow is known as the transition temperature. Because the mix becomes stiffer and more viscous as SBS concentration rises, Fig. 4.1 demonstrates that the softening point of SBS modified binder also rises. We can use asphalt grade by adding SBS in the hotter areas as in those areas if we will use a binder with a normal softening point value then the bitumen starts flowing at its softening point and will not properly coat the aggregates. Generally higher softening point indicates lower temperature susceptibility, and it is preferred in hotter climates.

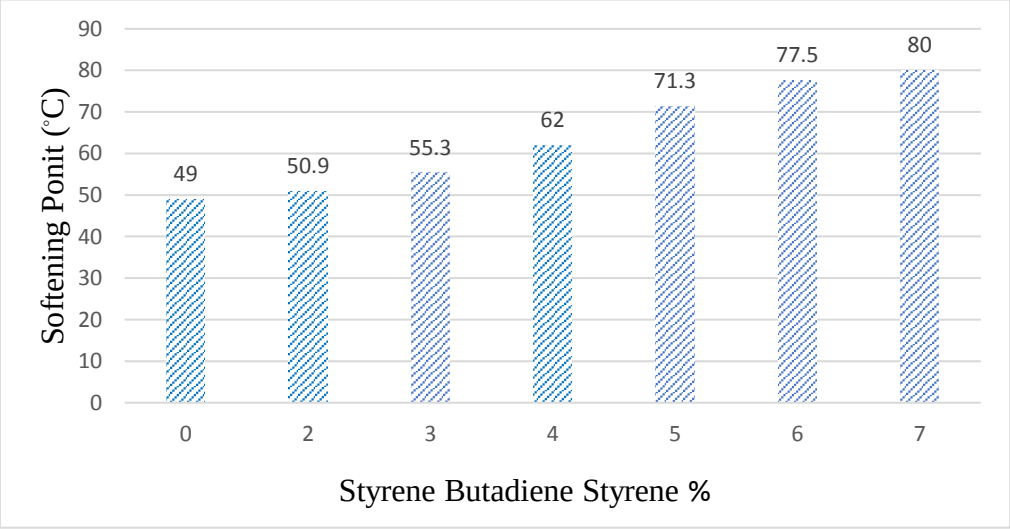

Figure 4.1: Measured Softening point of SBS Modified Asphalt

4.2.2 Penetration

The indication known as penetration refers to the asphalt binder's penetration grade (PG). Pakistan uses PG 40/50, 60/70, & 80/100 grades. According to NHA specifications, PG 80/100 will be utilized if the mean annual air temperature is less than seven degrees Celsius, PG 60/70 if it is between seven and twenty-four degrees Celsius, and PG 40/50 if it is over twenty-four degrees Celsius. As seen in Fig. 4.2, the SBS Percentage Since the mixture is viscous and hardened, the penetration value is declining. Penetration value at 0% SBS is 66 while at 7% SBS it is 45. Lower penetration levels indicate better consistency, whereas higher penetration values indicate softer consistency. As a result, only climates with a warmer to milder temperature may employ bitumen combined with SBS.

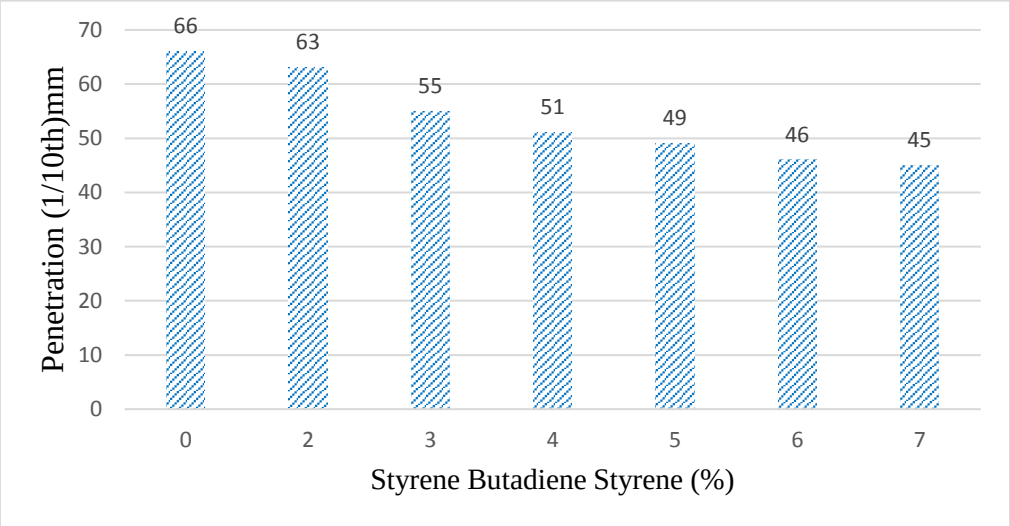

Figure 4.2: Measured Penetration of SBS Modified Asphalt

4.2.3 Ductility

A test index called ductility is used to describe how well an asphalt binder performs at low temperatures. The low-temperature fracture resistance will be better the higher the ductility. Similarly, more breaking of the binder mixture is caused by lower ductility. Figure 4.3 demonstrates that ductility will decrease when SBS increases. If an HMA bond is not sufficiently ductile, repeated traffic loads will cause it to break. In highway construction, a mix's value should never be lower than 50. In our analysis, the ductility value for a 7 percent SBS mix is 64 cm.

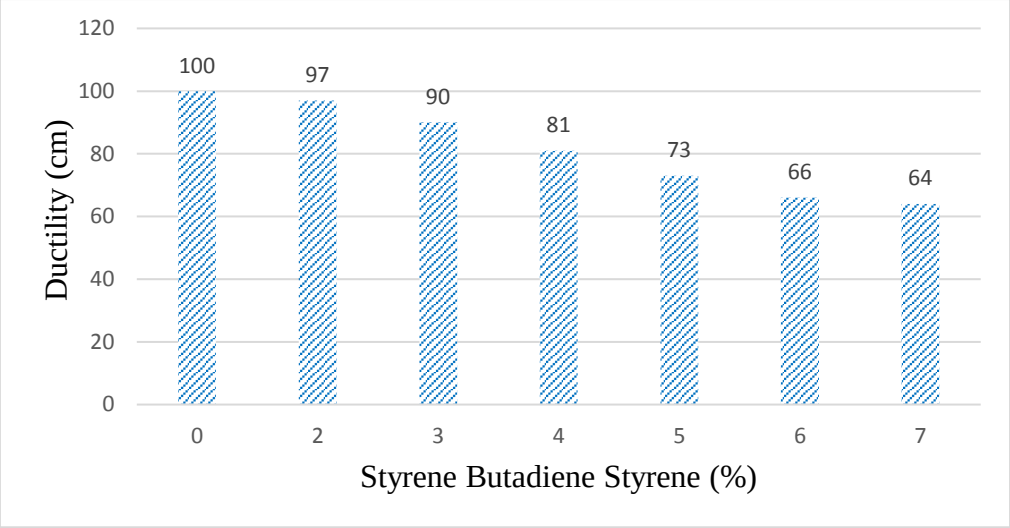

Figure 4.3: Measured Ductility of SBS Modified Asphalt

4.3 Dynamic Modulus Test Results

Testing specimens in the Simple Performance Tester at four distinct temperatures 4.4, 21.1, 37.8 & 54.4, and seven different loading frequencies 25, 10, 5, 1, 0.5, 0.1, & 0.01 Hz resulted in the Dynamic Modulus test results (SPT). Each SBS % was evaluated on three duplicate samples. With a rise in temperature and a reduction in loading frequency, the Dynamic Modulus values dropped for all SBS modified and unmodified samples. This indicates that |E*| at higher temperatures are more sensitive and vulnerable to mistakes, hence appropriate caution is needed when testing specimens at higher temperatures. It has been shown that the coefficient of variation for |E*| in most situations rose with an increase in temperature. To attain the proper temperatures, which should be verified before the test, specimens should be the condition for the necessary equilibrium periods.

4.3.1 Development of Mater Curves

To assist in pavement structural response design, the test findings were used to develop master curves. Utilizing the time superposition principle, a smooth, uniform curve that shifts each temperature to the reference temperature was used triplicate specimens have been tested at each temperature, and the desired frequencies at 21°C as a reference temperature and an average of those values were used to produce Master curves. As part of the NCHRP Project 9-29, a Master Solver Excel Sheet was used to build master curves The MS Excel solver add-in tool is used to decrease the sum of squared errors to fit the curve. Moreover, low frequency such as (0.1 Hz) shows low-speed traffic movement, while (25 Hz) is showing High-speed traffic movement so from the figure 6% SBS has optimum |E*|

for low and high-speed traffic at lower temperature and higher temperature such as 4.4°C & 54.4°C. All seven mixes' master curves are given in Fig. 4.4, which shows that lower frequencies separate them more than higher frequencies. Table 4.1 shows the fit statistics for each mix's master curves. A good model has an R^2 value greater than 0.7. The value of R^2 for 0% SBS is 0.97, whereas the value of R^2 for the optimal SBS modifier in this research, 6% SBS, is 0.86. This indicates that the addition of SBS alters the mechanical characteristics of the mix.

Table 4.1: - Goodness of Fit Statistics for Dynamic Modulus Curve

SBS %	R^2	Se/Sy
0	0.977	0.12
2	0.967	0.11
3	0.927	0.19
4	0.898	0.23
5	0.879	0.24
6	0.868	0.26
7	0.933	0.18

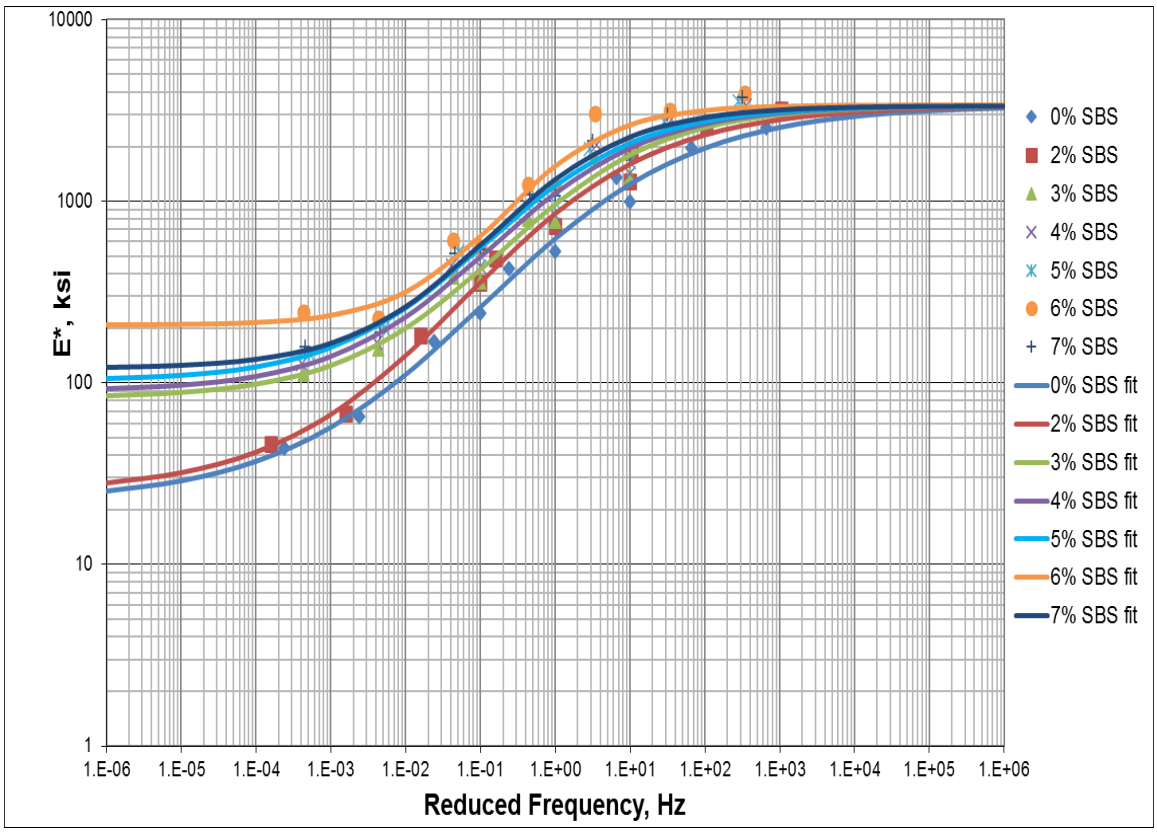

Figure 4.4: Master Curves for Dynamic Modulus |E*| for all Mixtures.

4.3.2 Dynamic Modulus for Two-Level Factorial Design

To examine how different variables interact with one another and with the dynamic modulus, a two-level factorial design approach is utilized. This technique is compatible with Minitab 1.6. All the mixing variables, such as NMAS, OBC, VMA, VFA, Test Temperature, and Frequency, are initially present. However, after running the test originally, the unimportant factors were left out to make things simple, and the significant variables are shown above. Table 4.2 lists the only levels that were taken into consideration for the study: High and Low.

Table 4.2: - Factors Considered in the Study for Two Factorial Design Process

Abbreviation	Factors	Units	Low Level	High Level
Freq	Frequency	Hz	0.1	25
Temp	Temperature	˚C	4.4	54.4
SBS	SBS	%	0	6

Due to the factorial design, the main and interaction impact are shown in Table 4.3. In factorial designs, the term "effect" refers to the difference in the average responses of any given component when it is at its high level compared to when it is at its low level. The term "interaction effect" refers to the mean difference between one factor's influence at a high level and another factor's effect at a low level. The factor's impact estimates are 2 times the matching regression coefficient in value.

Table 4.3: - Dynamic Modulus Main and Interaction Effects Estimate

One factor			Two factors			Three factors		
Main Factor	**Effects**	**p-value**	**Interaction**	**Effects**	**p-value**	**Interaction**	**Effects**	**p-value**
Temp	-12200	0	Temp*Freq	-7608	0	Temp* Freq*SBS	-3296	0
Freq	11981	0	Temp*SBS	1308	0			
SBS	2102	0	Freq*SBS	6827	0			

Table 4.3 demonstrates that changes in SBS and frequency have a greater impact on |E*| values since a positive sign indicates a causal link. Additionally, the effect-based arithmetic sign denotes the nature of the link. An inversely proportionate connection between a factor and the response variable, in this instance the dynamic modulus, is represented by an effect with a negative value, like temp in this example. The analysis was

done at a 0.05 level of significance. The factors with a p-value of 0.05 or less are thus considered significant and are included in Table 4.3. SBS, Temp, and Freq Given that their p-values are less than 0.05, the two-way interactions between temperature and frequency, temperature and SBS, and temperature, frequency, and SBS and three-way interaction were found to be significant.

The Analysis of Variance (ANOVA) for the measured data of |E*| up to three-way interaction effects is shown in Table 4.4. It denotes that there are three variables explaining the major impact Temperature, Frequency, and SBS.so, there are three degrees of freedom for the main effect. By comparing the p-value to 0.05 and the value of F, which is often larger than 10, the importance of a factor is assessed. Therefore, the main effect, two-way interaction, and three-way interaction are all regarded as significant since they have a large impact on |E*| and the P value is smaller, and F is also more than 10.

Table 4.4: - ANOVA for Dynamic Modulus

Source	DF	Sum of Square	Mean Sum of Square	F	P
Main Effects	3	1780898105	593632702	1228.50	0
2-Way Interaction	3	637146685	212382228	439.52	0
3-Way Interaction	1	65179257	65179257	134.89	0
Residual Errors	16	7731483	483218		
Pure Error	16	7731483	483218		
Total	23	2490955531			

The cumulative normal probability plot for the standardized main and interaction effects with a 95 percent confidence interval is shown in Fig. 4.5. The probability plot offers a clear view of the importance of many parameters. Dots in red and black indicate significant variables and those that are not. Temperature is on the negative side of the plot, which indicates that it has an inverse relationship to |E*|, while frequency and SBS are on the positive side and have a direct relationship to |E*|. This indicates that temperature and frequency together as well as temperature and SBS have a significant impact on dynamic modulus.

Fig 4.6 shows the main effect plot for |E*| which states that the main effect is plotted versus high and low levels of factors considered for the study and the sharp slope of the

line tells that there is a strong relation between parameter and response variable. Main Plot shows that Temperature, Frequency, and SBS have sharp slope line depicting Temperature as a significant variable affecting |E*| inversely while Frequency and SBS is also significant variable affecting |E*| directly.

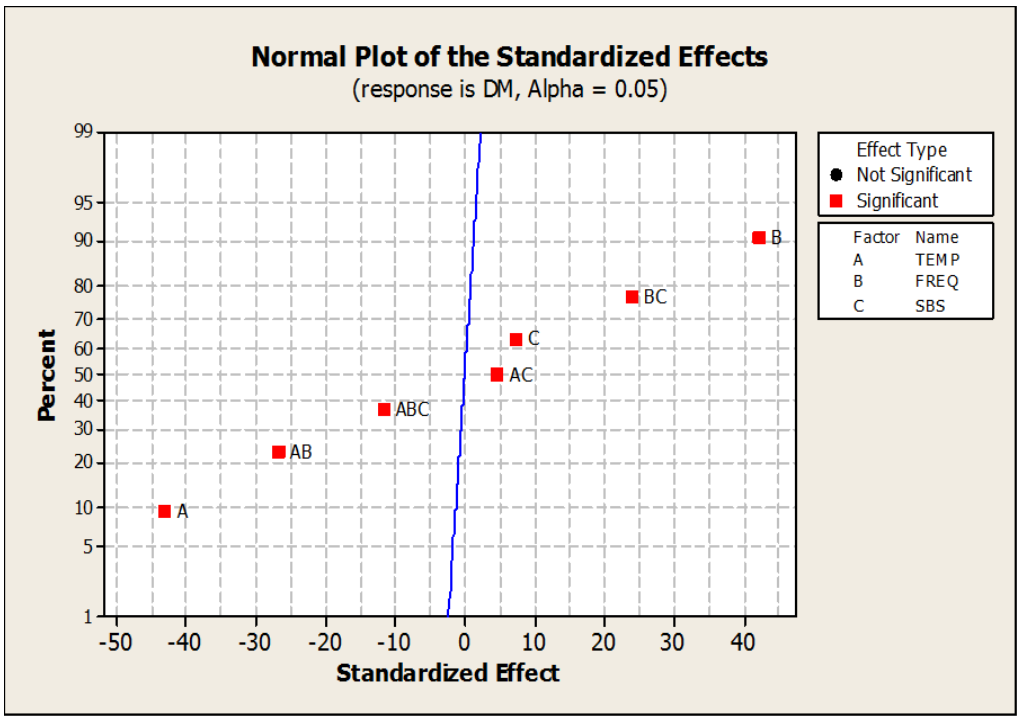

Figure 4.5: Cumulative normal plot for Dynamic Modulus

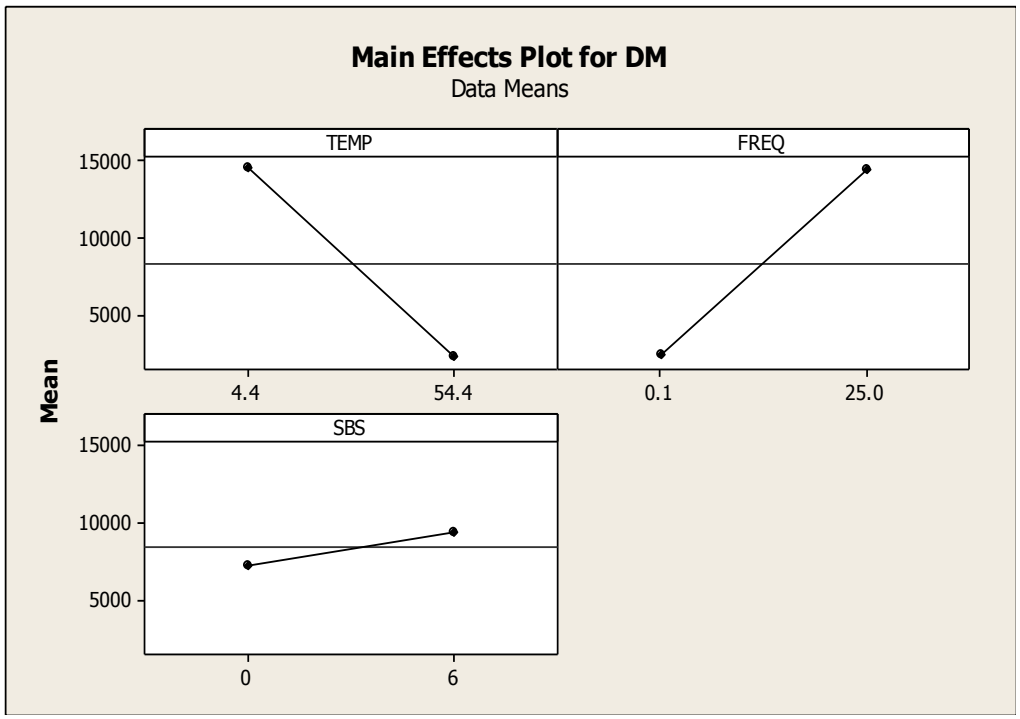

Figure 4.6: Main Effects Plot for Dynamic Modulus

Dynamic Modulus signifies when one element fails to have the same impact on responses at varying levels of some other component, as seen in the figure. Fig.4.7. When one variable is changed, the influence of the other changes, which is when two variables interact. The importance of the interaction effect between the factors is shown by non-parallel lines, which signifies that negligible factor interactions generate comparable patterns in the response at different levels of a different factor and vice versa. The intensity of the interaction, in this example temperature, is expressed by the steepness of the line slope. Because there is no parallel line in the figure below, there is a strong interaction between the parameters of temperature and SBS and frequency and temperature. As a result, |E*| is significantly affected by these three factors.

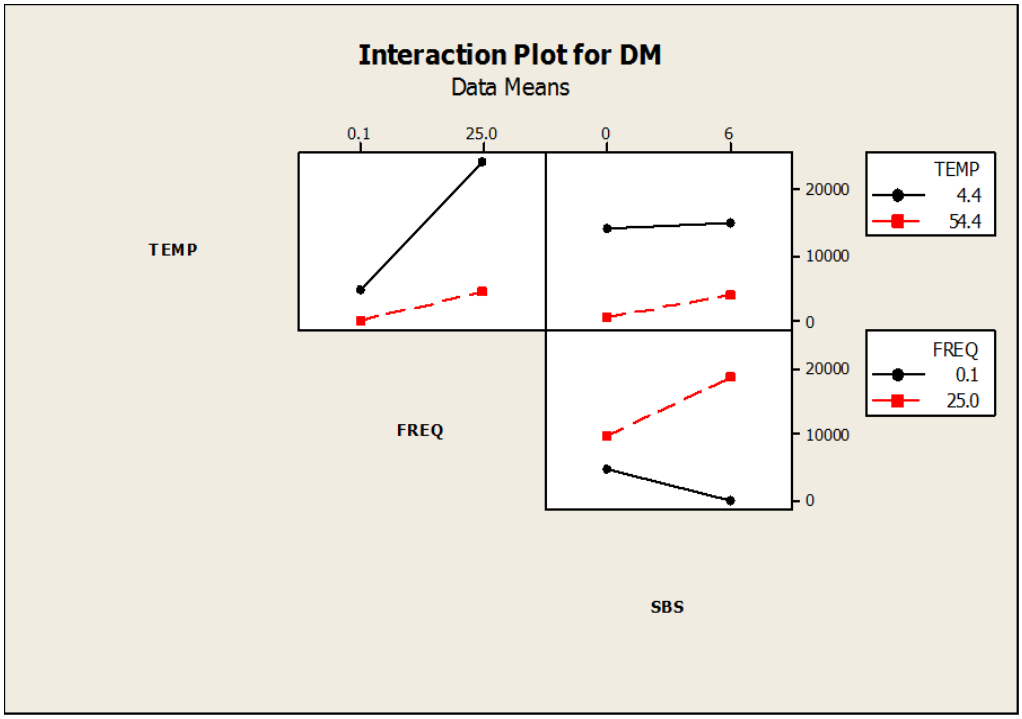

Figure 4.7: Plot of Dynamic Modulus Interaction Effects

Using a Pareto chart, Figure 4.8 illustrates the importance of the factor effect and the interaction effect. The fact that the bars in this figure cross the t-critical value for the 95 percent confidence interval shows that temperature, frequency, and SBS are important characteristics that influence the value of |E*|. On the other hand, the bars that are hidden beneath the reference lines show that although the individual effects of the variables do affect |E*|, the interaction effect of the factors does not significantly affect |E*|. A Pareto chart may be used to understand the importance of each component as well as how they relate to one another. Additionally, it shows the relative importance of the component

impact, also known as the standardized effect, which is the combination of components for the mean response and the specified threshold of significance, in this case, 5%. To show that lines in the plot that cross the reference line are significant whereas lines that do not cross the reference line are not, a T-critical reference line is drawn. As their bars also cross the reference line, temperature, frequency, temperature and SBS, and other factors all significantly affect the value of |E*|.

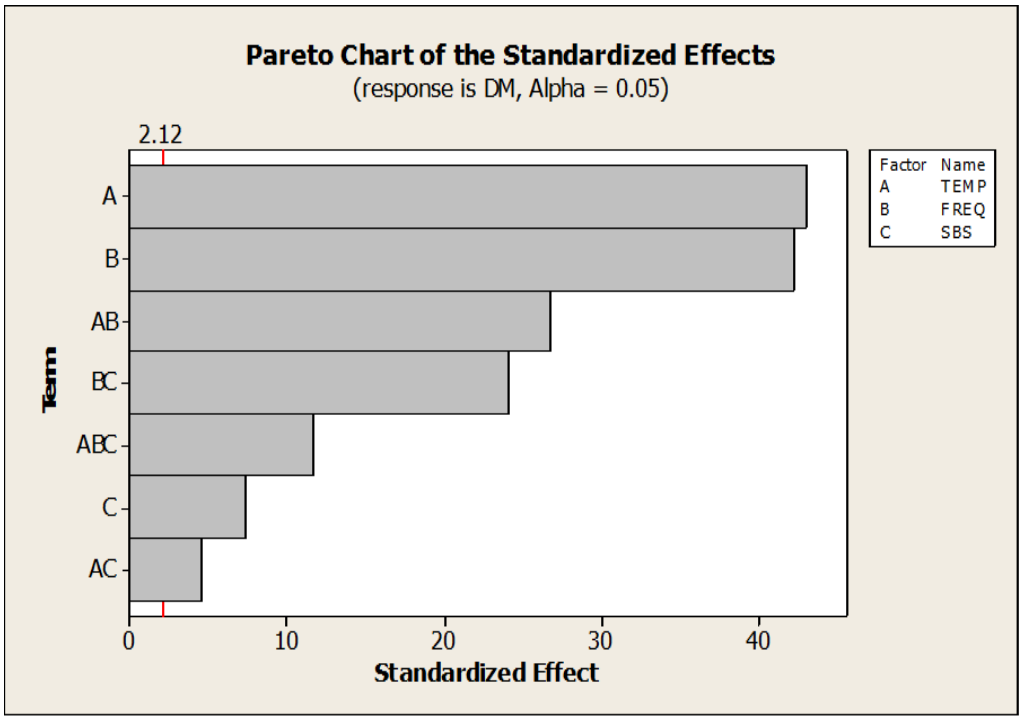

Figure 4.8: Dynamic Modulus Pareto Chart

The cube plot in Figure 4.9 clearly shows that at 4.4 C and 25 Hz, the greatest value of |E*| is reached. Due to the material stiffening and resulting in reduced strain, the tendency to raise |E*| may be attributed to this. But on the other hand, at 54.4 C and 0.1 Hz, the minimum |E*| is achieved. This is due to the fact, that the material would become flexible and produces more strain, which ultimately reduces the |E*|. According to this figure, Temperature, Frequency, and SBS all have a substantial influence on the amount of |E*|.

A contour plot is a crucial tool for interpolation, which establishes the necessary response values at any value based on the factor. Figures 4.10 and 4.11, respectively, response/contour plots for SBS percentages of 0 and 6 correspondingly. This graph shows that the value of |E*| increases with frequency but decreases with temperature. Like a topological map, but with each line denoting a distinct contour with the same dynamic modulus. You may get |E*| by tracing a line over the contour plot with the frequency axis

parallel to it. A straight line drawn perpendicular to the vertical axis may be used to compute |E*| at any temperature if the frequency is maintained.

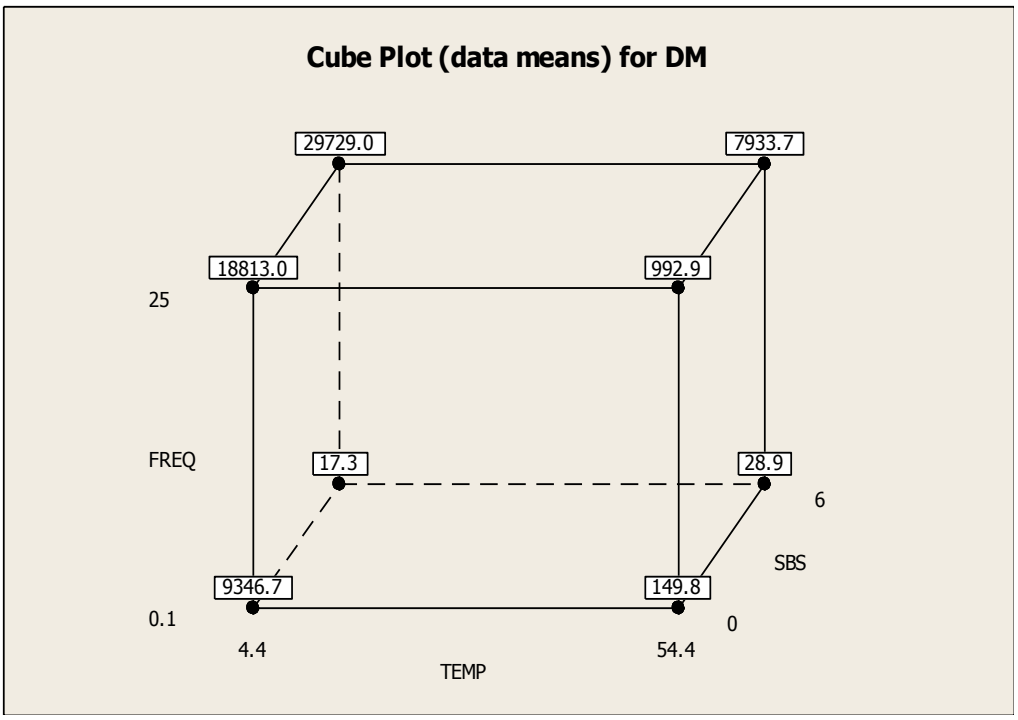

Figure 4.9: Cube Plots for Dynamic Modulus

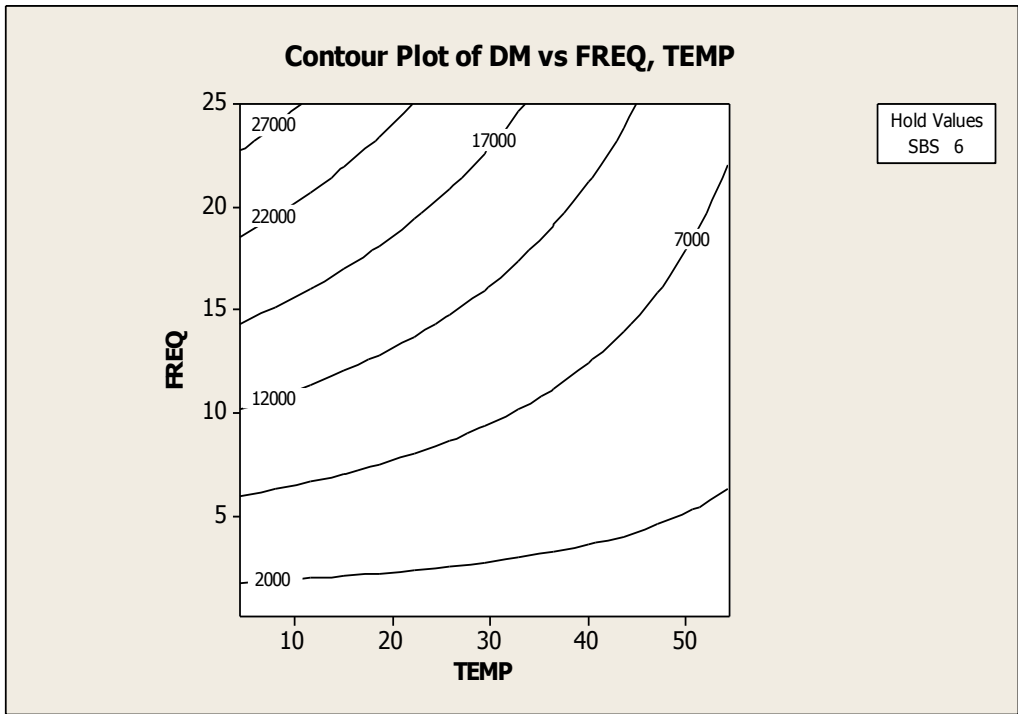

Figure 4.10: Contour Plots for Dynamic Modulus at SBS 6%

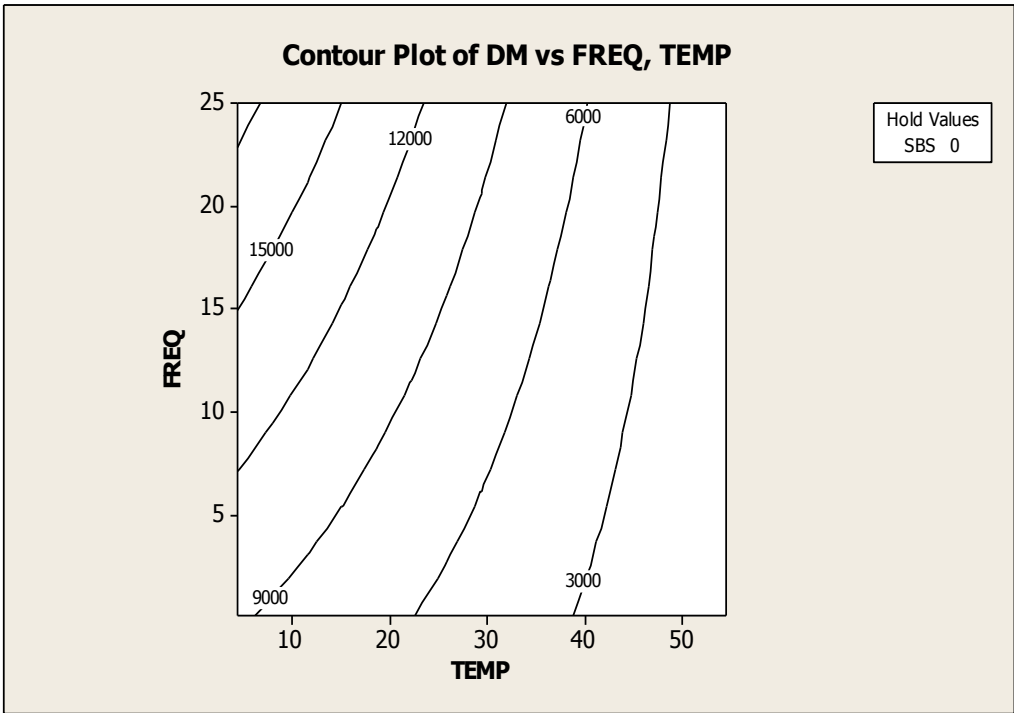

Figure 4.11: Contour Plots for Dynamic Modulus at SBS 0%

4.3.3 Performance Modelling

The pavement's performance under various situations, such as temperature, loading, and weather, is measured by the pavement's performance. The creation of models to foresee distresses like cracking and fatigue is the foundation of the mechanistic portion of the newly created AASHTO 2002 M-EPDG design guide. For a long pavement life, it is crucial to anticipate pavement performance at the design stage. In this instance, the performance indicator |E*| is dependent upon the volumetric characteristics of the mix, the loading frequency, and the test temperature. For the creation of the model for the |E*| finding, the data from laboratory tests are employed. Cobb-Douglas general form is used in cost-based empirical investigations to illustrate the effect of two or more inputs with various functional forms. An equation may be used to represent the functional version of the Cobb-Douglas model for this research investigation Equation (4.1).

$$|E^*| = \alpha T^{\beta 1} \times F^{\beta 2} \times S^{\beta 3} \qquad \text{Equation 4.1}$$

Where,

α, $\beta 1$, $\beta 2$, $\beta 3$ = Regression Coefficients

T = Temperature, Degrees (4.4 to 54.4 $^{\circ}$C)

F = Loading Frequency, Hz (0.1 to 25 Hz)

S = SBS in Percentage

The model for the SBS unmodified and modified mixes utilized in the research is developed using a non-linear regression analysis technique. Multiple linear regression was first employed to create the model, but since it did not provide a satisfactory coefficient of determination (R^2), nonlinear regression was selected instead, which more effectively suited the data. The overall model was created using SPSS software and nonlinear regression. Table 4.5 displays the parameter statistics.

Table 4.5: Model for nonlinear regression Summary

Parameter	Estimate	Std Error	T-Stat	R^2 (%)	95% Confidence Interval	
					Upper Bound	Lower Bound
β1	-0.691	0.036	-19.19	79.4	-0.620	-0.763
β2	0.122	0.015	8.13		0.152	0.092
B3	0.222	0.064	3.468		0.348	0.097
A	37963.633	4551.082	8.34		46949.902	28977.365

Table 4.5 displays the model's statistics and parameters. If the R^2 is larger than 0.7, the model is good and approved since it captures 79 percent of the variance in |E*|. All independent variables have a significant critical value of t-stat at a 95 percent confidence interval, i.e., 2.3808. The final version of the SBS modified model can be written as

$$E^* = 37963.633 \times T^{-0.691} \times F^{0.122} \times SBS^{0.222} \quad \text{Equation 4.1}$$

4.3.4 Model Validation

Model validation measures the regression model's ability to predict observed data. Measures are used to evaluate the predictive power of regression models. In this study, the difference between the observed and estimated data values is divided by the observed value, resulting in a mean absolute percentage error (MAPE). By multiplying the mean absolute error by 100, we can calculate the mistake as a percentage.

$$MAPE = \frac{100\%}{n} \sum_{i=1}^{n} \frac{|At - Ft}{At} \quad \text{Equation 4.3}$$

Where,

Ft = Fitted Value

At = Actual Value

The MAPE of the model employed in our research is 9.12%. Figure 4.12 depicts the model's validation plot. The higher the model's predictive performance would be if it

had more data values around the 45 ° line, and it is clear from the figure that many of the data values are near the line, indicating that the model is excellent.

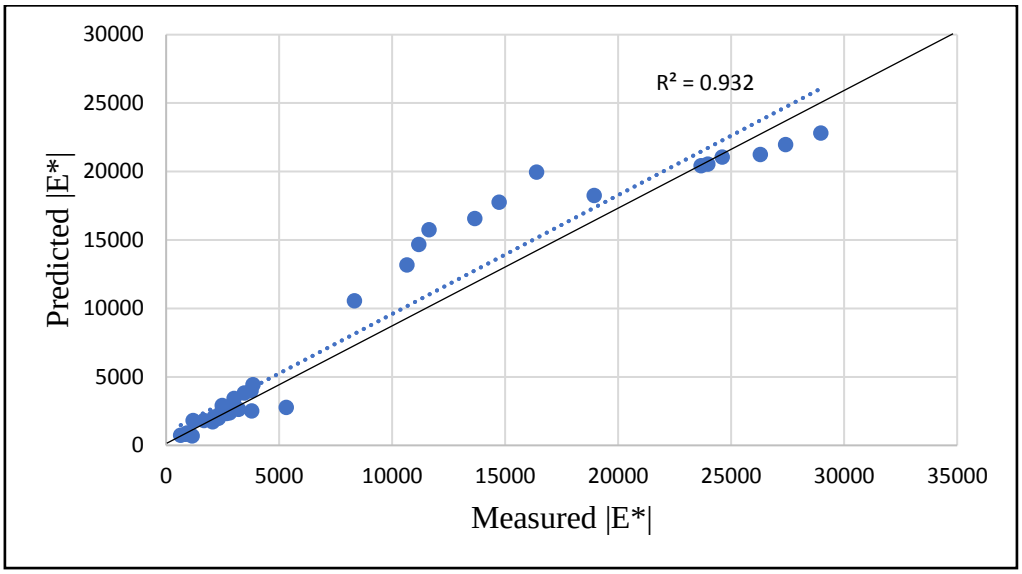

Figure 4.12: Validation Plot

4.3.5 Multi Expression Programming (MEP) using Artificial Intelligence (AI)

A Genetic Programming technique called MEP employs a linear depiction of chromosomes. MEP individuals are collections of genes that encode sophisticated computer programmes. Expressions encoded by MEP people are represented similarly to how compilers convert C or Pascal expressions into machine code. The capacity of MEP to store many answers to an issue in a particular nucleotide is a special property. For a fitness task, the best option is often picked. When addressing issues involving symbolic regression or categorization. One parsing of the chromosome is sufficient to evaluate the expressions encoded into an MEP person. Crossover and mutation offspring are always MEP individuals with the proper syntax (computer programs). Therefore, no further processing is required to mend recently acquired persons. Speeding up use of SBS in the construction industry requires the application of cutting-edge machine learning techniques and MEP to predict the |E*| at different temperatures and the SBS content. The unique encoding property of the MEP allows for the encapsulation of several equations (chromosomes) in a single programme. The final replication of the issue is picked from among the finest of the chosen chromosomes. In contrast to other machine learning techniques, MEP does not need knowing the final equation in advance. After the MEP has evolved, any mathematical mistakes in the final phrase are checked for and fixed. When compared to other soft computing systems, MEP's decoding process is straightforward. Even though MEP has

several significant benefits over many other algorithms, its application to civil engineering is limited.

Table 4.6: MEP hyper-parameter for SBS modified HMA

MEP hyper-parameter	SBS Modified HMA
Subpopulations Number	50
Subpopulation Size	500
Code Length	50
Cross Over Probability	0.9
Mutation Probability	0.01
Cross Over Type	One-Cutting Point
Number Generations	500
Total runs	10

In material engineering settings, for example, where a little change in an asphalt pavements variable might have a large effect on Hot Mix Asphalt stiffness and dynamic modulus, MEP is useful since the uncertainty in the target equation isn't immediately apparent. Numerous solutions exist for a linear chromosome in MEP, allowing the software to make an educated guess by considering a wider range of possible locations. To kick off the MEP modelling for the SBS Modified HMA, we settled on a subpopulation size of 500. Table 4.6 provides a summary of the MEP modelling hyper-parameters that have been selected.

$$E^* = \left(\left(\left(\frac{64-F}{\sqrt{T}}\right)+\left(\frac{4096}{2F}\right)+\frac{64}{F}+S\right)+\left(64ST+\left(\frac{8192S^2T^2-32768S^2T}{F^2}\right)\right)\right.$$
$$+\left(16384+4F^2-512F+\left(\frac{4096S}{F^2}\right)\right)$$
$$\left.+\left(64-F*\left(\frac{64}{F}+S-2T-4-\left(\frac{64-F}{\sqrt{T}}\right)\right)\right)\right)$$

Where,

T= Temperature in ˚C, F= Frequency, S= SBS, E*= Dynamic Modulus

The basic arithmetical processes of multiplication, division, addition, and subtraction were considered to build an optimum equation that is simple and easy. How accurate the model is before process is ended depends on how many generations were utilised to construct it. A programme with more generations would result in better results with less error. Utilizing cross-over and mutation rates, it is also feasible to determine the probability that children may experience genetic functions. The combination that produced the best outcomes out of many combinations was selected. It's important to remember that a model's accuracy is influenced by how long it takes to develop. The model's development never ends as new variables are included into the setup. Contrarily, this research hypothesises that 500 generations mark the end of starting to change or the threshold at which the fitness function alters by less than 5%. Equation 4.6 refers to the Final MEP model for calculating the dynamic modulus of SBS Modified HMA. MEP model validation for SBS modified HMA R^2 is 96.67 percent in Figure 13.

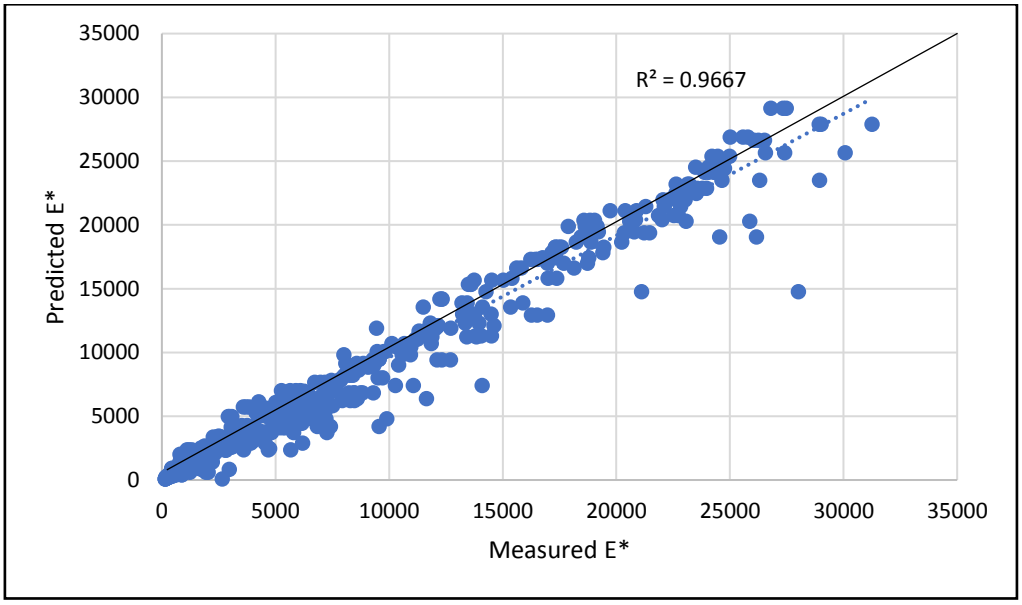

Figure 4.13: MEP Model Validation for SBS Modified HMA

4.3.6 Sensitivity Analysis

Sensitivity analysis is used to explain how various independent variables (Inputs) affect the dependent variable (Output) under a predetermined set of circumstances. Sensitivity analysis indicates how sensitive the output is to certain input variables or changes in the input parameters. This study is carried out under defined limits conditions that will specify for input variable. It may be particularly helpful when evaluating how well models or outputs hold up when different input parameters are used. Temperature and

frequency serve as the study's input parameters, while the dynamic modulus serves as the study's result.

According to the test findings, the dynamic modulus has an inverse relationship with test temperature, which indicates that as temperature rises, the dynamic modulus eventually falls, and vice versa. The opposite phenomenon is seen when frequency falls, which lowers the dynamic modulus values. Testing at higher temperatures necessitates great care and the samples must be maintained to condition for a such required period at equilibrium, as evidenced by the significant variation in dynamic modulus results. This implies that the test is highly sensitive to and prone to errors at higher temperatures. Once the proper temperature has been maintained for the necessary amount of time, the test should be performed.

Using isothermal and isochronal curves, we can see whether the average value of |E*| has risen or fallen as a function of testing temperature and loading frequency. As shown in Fig. 4.14, the value of |E*| decreases as temperature rises while rising as frequency rises. Since |E*| is the ratio of stress to peak recoverable strain, it is higher at lower temperatures than at other temperatures because the strain is temperature-sensitive, increasing stiffness in colder temperatures while increasing flexibility in warmer ones. Since the mix was stiffer and less likely to deform under stress, it had a greater dynamic modulus of 6 percent SBS.

The stress-strain relationship in Fig. 4.15 demonstrates that |E*| increased with higher frequency or with an increase in frequency. At higher loading frequency, decreased tire-to-pavement contact time/pressure results in a rise in |E*|. The graphs reveal that SBS 6 percent has a greater |E*| than 7 percent, which is also the optimal SBS percent advised in this research for a combination to attain a higher |E*|. Higher temperatures have a lower |E*| because they are more prone to errors and strain, both of which are exacerbated by temperature and flexibility.

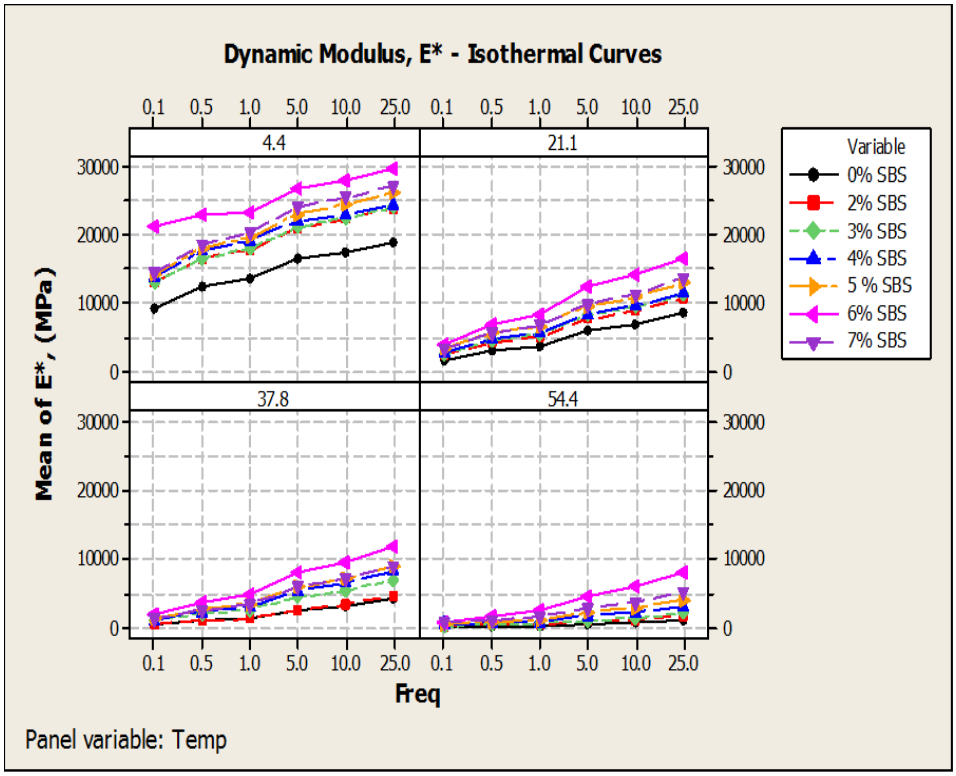

Figure 4.14: Dynamic Modulus-Isothermal Curves

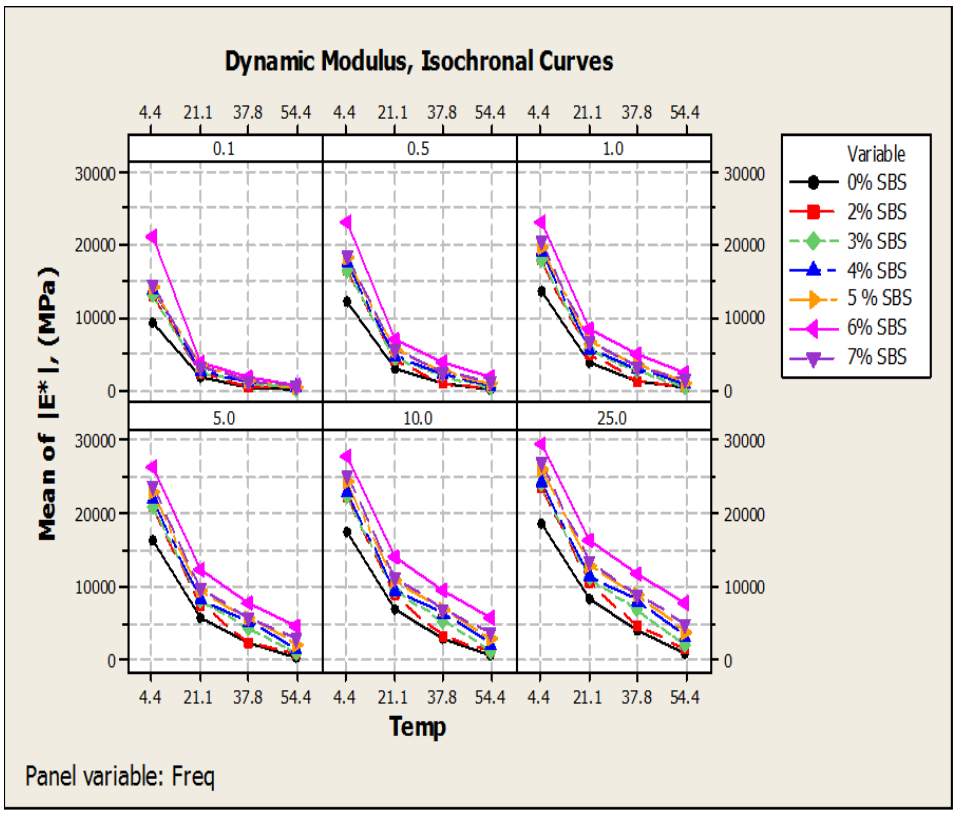

Figure 4.15: Dynamic Modulus-Isochronal Curves

4.4 Phase Angle

The phase angle is the angle at which compressive stress lags the axial strain. From obtained results, that phase angle initially rises with temperature and falls with frequency. On the other hand, the phase angle exhibits opposite behavior and starts to decline with a rise in temperature and drops with a reduction in frequency; yet this appears to be judged fit until temperature surpasses 37.8°C. Figure 4.16 is a good example of this pattern. From the figure, it is obvious that the phase angle first rises with temperature but then begins to decline. The fact that phase angle increases dynamic modulus at lower temperatures shows that most of the energy is due to HMA's viscoelastic nature. The binder has the most impact on the phase angle of asphalt mixes. As a result, it adheres to the binder's phase angle trend. The phase angle for asphalt mixes, however, falls with decreasing frequency or rising temperature due to the aggregate impact, and more energy is lost in viscoelasticity since the aggregate mostly influences the phase angle at low frequency and high temperatures.

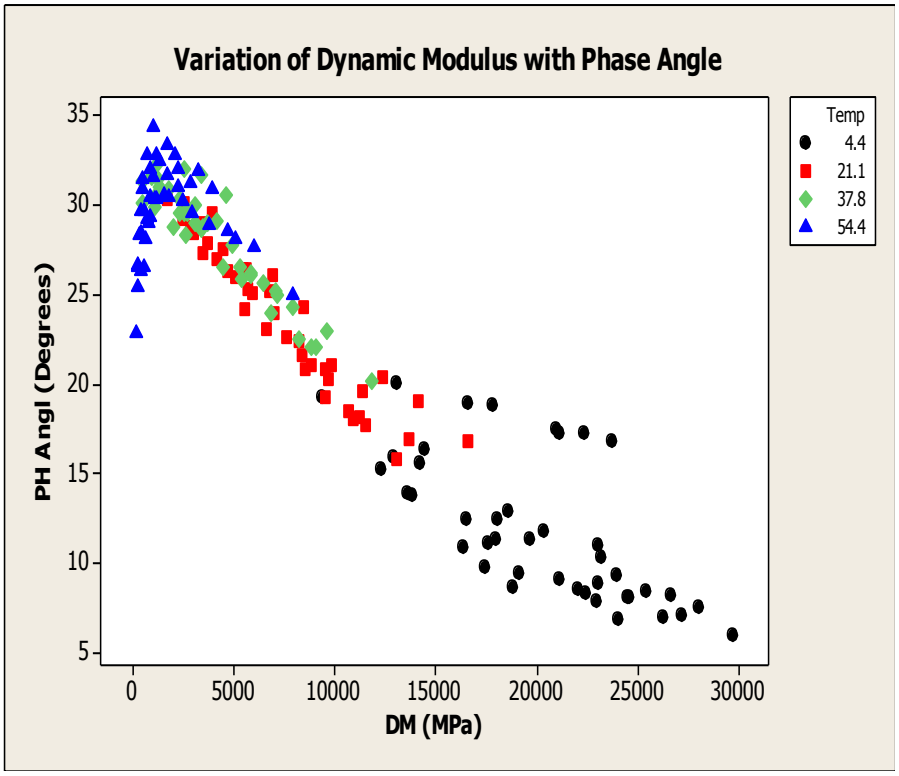

Figure 4.16: Variation of Dynamic Modulus with Phase Angle

4.4.1 Phase Angle Factorial Design Using Two Level Factorials

Phase angle factorial design follows the same technique as |E*| factorial design. In this case, phase angle serves as the response variable. SBS, frequency, and temperature all have substantial effects on phase angle, as shown in Table 4.7's impact estimates for phase

angle. The temperature has an arithmetic sign that is directly proportional to phase angle, but frequency and SBS have a negative sign that is inversely proportional to phase angle. There is also no significance in the two-way interaction of temperature & SBS, temperature & Frequency and frequency & SBS, since their p-value is more than =0.05, and the three-way interactions are likewise significant because their p-value is lower than =0.05

Table 4.7:Phase Angle Main and Interaction Effect Estimates

One factor			**Two factors**			**Three factors**		
Main Factor	Effects	p-value	Interaction	Effects	p-value	Interaction	Effects	p-value
Freq	-2.748	0	Temp*Freq	6.674	0	Temp* Freq*SBS	-0.146	0.170
Temp	15.343	0	Temp*SBS	-0.901	0			
SBS	-4.623	0	Freq*SBS	0.959	0			

Table 4.8 displays the results of the phase angle analysis of variance (ANOVA). The table shows that the main effect and the two-way interaction, are significant while three-way interactions are insignificant, as shown by a greater value of F than 10 and a lower value of P, respectively. Three elements (Temp, Freq, and SBS) are influencing the Phase Angle response, which has a degree of freedom of three.

Table 4.8: Phase Angle ANOVA

Source	DF	Sum of Square	Mean Sum of Square	F	P
Main Effects	3	1585.85	528.62	8547.91	0
2-way interaction	3	277.66	92.55	1496.60	0
3-way interaction	1	0.13	0.13	2.076	0.170
Residual Errors	16	0.99	0.06		
Pure Error	16	0.99	0.06		
Total	23	2047.52			

Figure 4.17 depicts the primary impacts of the variables affecting the phase angle graphically. A considerable influence on the response, i.e. phase angle, can be seen in the distance from the normal line for all three components, i.e. temperature, frequency, and SBS The phase angle is more dependent on that component which is far from the normal line It can be seen from Fig 4.17 that temperature has the most significant influence directly

on phase angle, while frequency and SBS has a considerable effect on phase angle, which are influencing inversely an also significant as shown by red dots in the plot. Two-way interaction is also significant while three-way interaction is insignificant.

Figure 4.18 represents the main effects plot and shows the importance of factors affecting the phase angle. Using the slope of the line, we can see how closely temperature, frequency, and SBS are related to the dependent variable, which in this case is the phase angle. The sharpness of the line's slope may be used to determine the relationship between a component and its response. The temperature has the greatest impact on phase angle, whereas Frequency & SBS seems to affect considerably phase angle since the line has a very low slope.

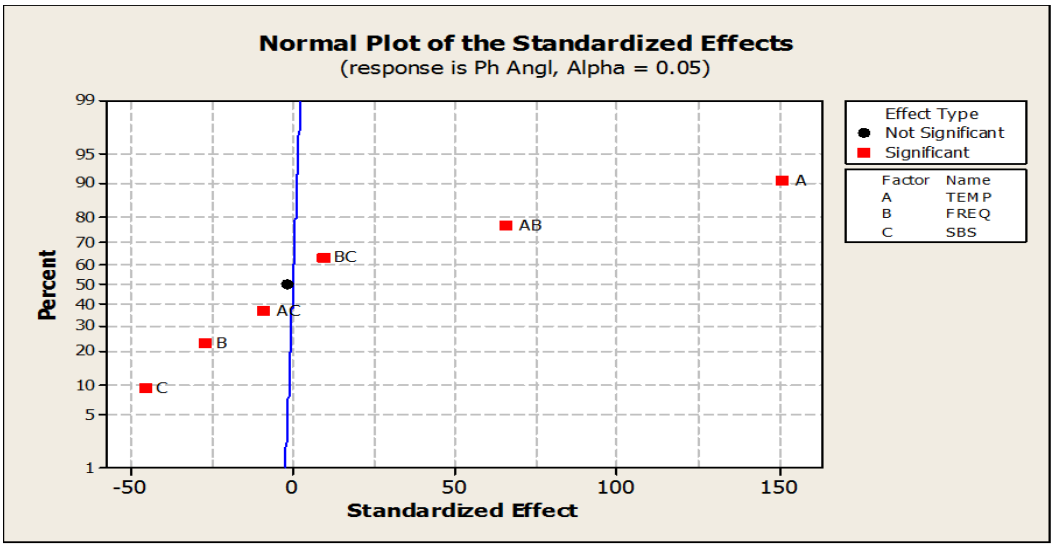

Figure 4.17: Phase Angle Normal Plot

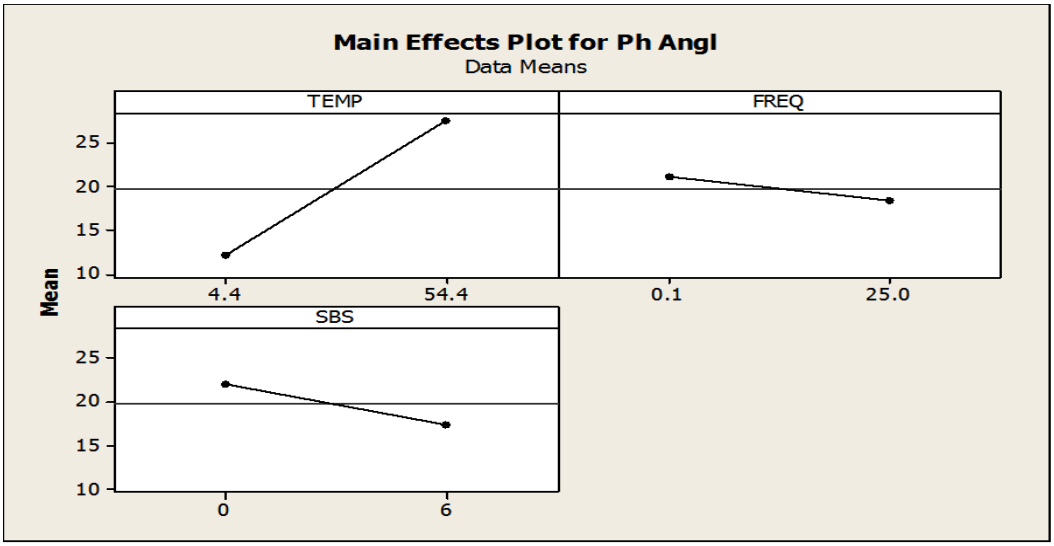

Figure 4.18: Main effects plot for Phase Angle

Figure 4.19 shows the interaction plot. the phase angle is affected by temperature, SBS and frequency as shown by the non-parallel lines. Therefore, all the interactions are significant.

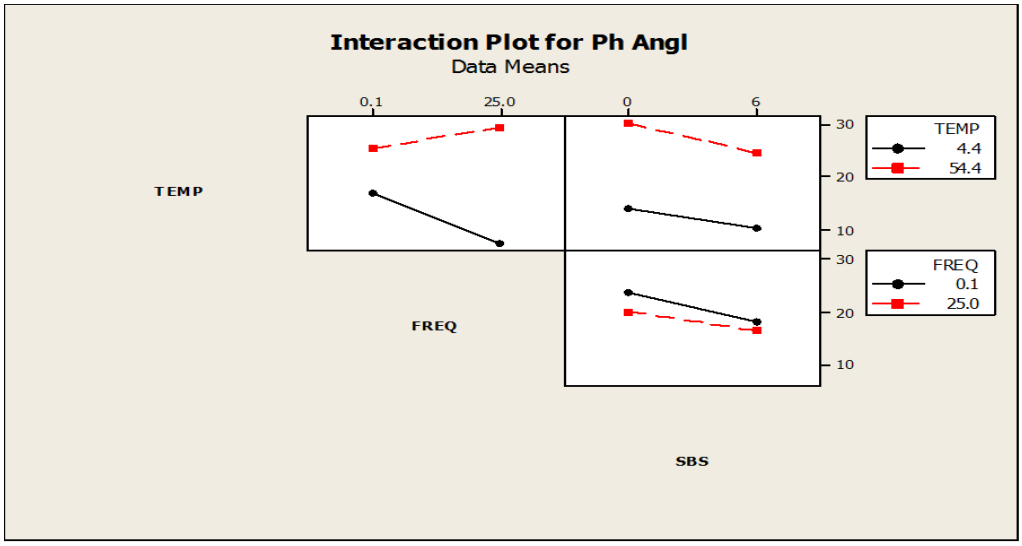

Figure 4.19: Interaction effects plot for Phase Angle

Fig 4.20 shows the Pareto chart for phase angle, which indicates the significance of variables. It is clear from the figure Temperature, SBS, and frequency bar cross the reference line individually, and all are significant. On the other hand, SBS, Frequency & Temperature jointly does not influence the phase angle since the bar does not cross the reference line and conforms to the primary effect plot in this experiment. When the temperature and frequency bars cross the reference line in a two-way interplay, they have a considerable influence on phase angle.

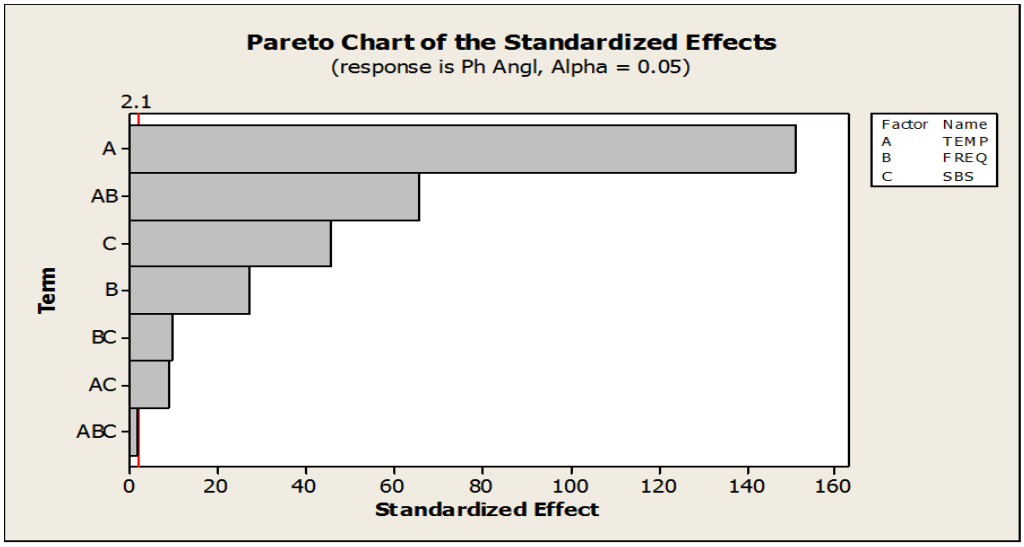

Figure 4.20: Phase Angle Pareto Chart

When finding the maximum phase angle to a given temperature and frequency, a cube plot becomes very useful. It is clear from figure 4.21 that the lowest phase angle is achieved at 4.4˚C at 25 Hz frequency and the highest phase angle is achieved at 54.4˚C at 25 Hz.

Isochronal and isothermal curves are the best representations of the relationship between phase angle and frequency and temperature. At temperatures of 4.4 °C and 21.1 °C, the phase angle rises with decreasing frequency, but at 37.8 °C and 54.4 °C, the phase angle decreases significantly. Lower temperatures tend to favor the elastic component, whereas higher temperatures are more likely to favor the viscous component in blends. Fig 4.22 shows that 0 percent SBS mix has a larger phase angle at every temperature & frequency because they include more bitumen than other mixes, which results in a higher phase angle and less temperature decrease.

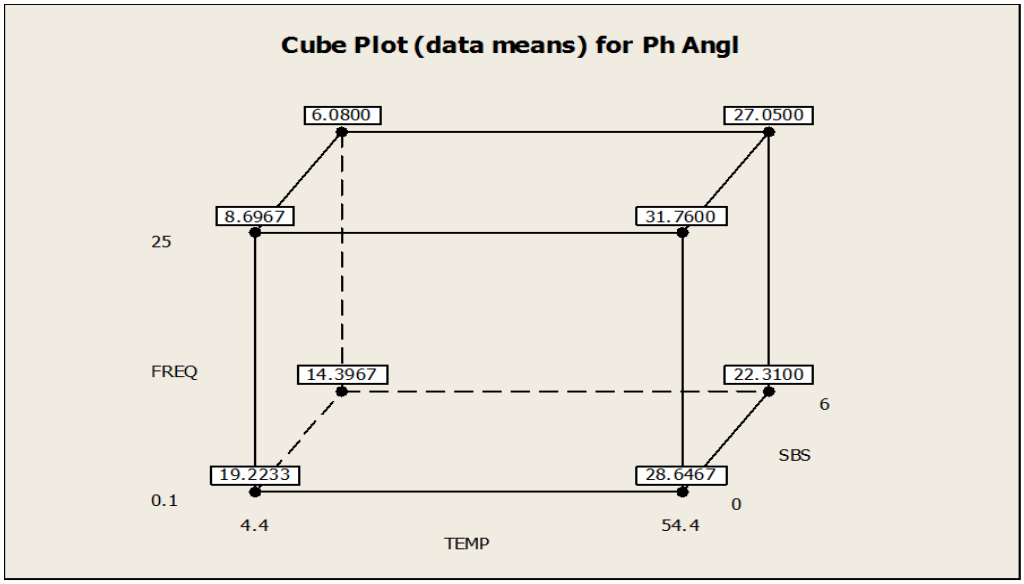

Figure 4.21: Cube Plot for Phase Angle

Fig 4.23 shows isochronal curves which show the variation of different temperatures at a single frequency 0% of SBS is showing a higher phase angle at all frequencies and tends to decrease at a higher frequency. Overall 0% SBS is showing more phase angle due to the highest binder content than other mixes. The phase angle increases from 4.4 C to 37.8 C before decreasing at frequencies of 0.1 Hz, 0.5 Hz, and 1 Hz. However, at 5 Hz, 10 Hz, and 25 Hz it rises as the phase angle tends toward the elastic part at temperatures lower and the viscous part at the higher temperature.

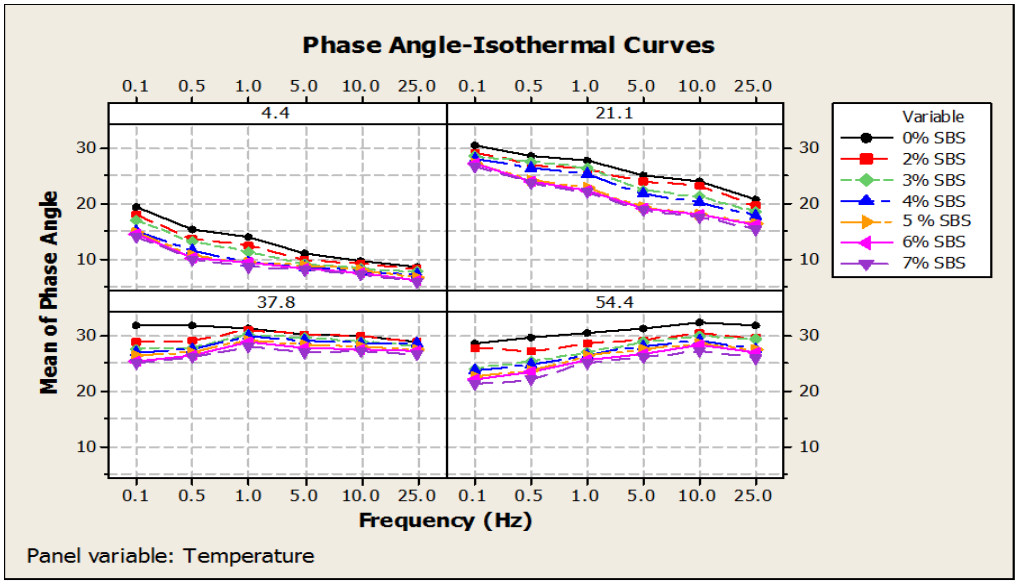

Figure 4.22: Isothermal Curves for Phase Angle

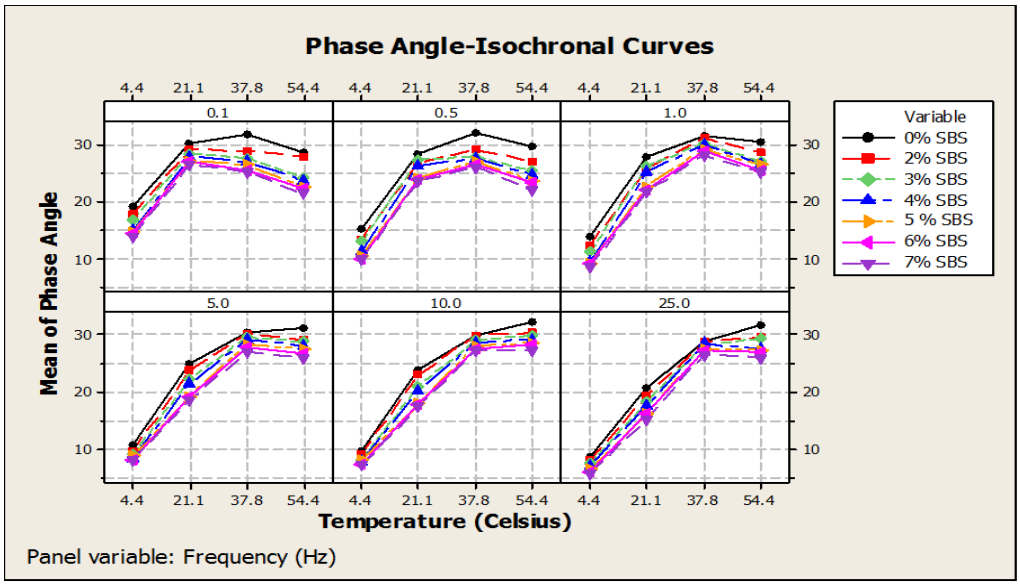

Figure 4.23: Isochronal Curves for Phase Angle

4.6 Summary

The results of the laboratory test on the SBS Modified and unmodified samples for the penetration test reveal that the penetration value falls as the SBS percentage rises. SBS percent was raised, raising Softening Point. SBS percent increases result in a fall in the ductility value. Following analysis of the laboratory test findings for |E*| and Phase angle, several charts are shown below. E* master curves were generated for each combination using the mean E* values obtained from dynamic modulus tests performed at various temperatures and frequencies. The E* values at each temperature were converted to 21.1°C, which served as the reference temperature. This was achieved by determining a lower

frequency that corresponded to each data point that needed to be moved to the reference temperature. Utilizing the time-temperature superposition concept, the impact of a temperature change is stated in terms of a frequency change. The input data used by M-EPDG for the chosen mixture types was created using Master Curves for each mix generated in the research.

To ascertain the impact and interactions of various factors that influence |E*|, a two-level factorial design has been used. The elements considered include temperature, loading frequency, and SBS It has been shown that |E*| values are significantly influenced by temperature, frequency, and SBS The interplay between temperature and frequency has a similar impact. To determine the major and insignificant effects on |E*| and phase angle, factorial plots were designed, including cumulative standardized, Pareto chart, and cube plot. Both SBS modified and unmodified mixtures are produced using the dynamic modulus predictive models. Their statistics are also shown in tabular form, and the accuracy of the model's prediction is examined by computing the mean absolute percentage error (MAPE) , Model validation by nonlinear regression analysis and Model validation by MPEX and comparing the fitted and observed data using a plot.

Additionally, sensitivity analysis is performed on the findings of the dynamic modulus test. Isochronal curves are plots where the panel variable is the frequency, and all temperatures are shown in a single panel as opposed to isothermal curves where the panel variable is temperature. These figures suggest that whereas frequency has a direct relationship with dynamic modulus, the temperature has an inverse relationship with it. As a result of the asphalt mixture's tendency to be stiffer at lower temperatures, where the contact and interlocking of the aggregate is the primary source of low dynamic modulus values, it is also noted that the dynamic modulus is greater at lower temperatures. The curves and bar chart illustration demonstrate the increased dynamic modulus of the SBS-containing mix (6 percent) compared to other mixtures. Contrarily, a mix with 0% SBS has larger phase angles than other mixes because they are more viscous owing to increased bitumen content.

Chapter 5

CONCLUSIONS AND RECOMMENDATIONS

5.1 Introduction

The study's primary goal was to determine the mechanical properties of SBS modified and unmodified mixtures to find the efficiency of SBS in HMA Bitumen penetration grade 60/70 obtained from ARL and SBS has been imported from Shijiazhuang Tuya Technology Co, Ltd China and used as 0%, 2%, 3%, 4%, 5%, 6%, and 7% to the weight of bitumen that was mixed with the high shear mixture at 180°C and a speed of more than 1500 rpm (Penetration, ductility & Softening Point). The Superpave Gyratory sample is prepared using the modified binder for the Dynamic Modulus Testing that was carried out by SPT.

Three replication specimens were subjected to the dynamic modulus test at temperatures ranging from 4.4 to 21.1 degrees Celsius and loading frequencies ranging from 25 Hz to 1 Hz. Testing in labs yielded dynamic modulus data, which was employed in statistical analysis that took into consideration temp, frequency, and SBS variables. For both the modified and unmodified SBS mix, the main and interaction plot, Pareto chart, and cube plot were used to further elucidate the main and interaction effects. Using the time-temperature superposition approach, the master curves were created at the reference temperature of 21°C. The temperature is moved to the reference temperature regarding the loading frequency using this technique until a smooth curve is formed. Excel's master solver sheet was used to do this. According to AASHTO TP 62-07, executing the test at a temperature of -10°C is necessary for the dynamic modulus test and the construction of master curves, however, this test cannot be carried out since SPT is unable to do the test. To build master curves, an extra frequency of 0.01 Hz at 37.8°C must be added to the spread sheet. The creation of master curves aids in Pakistan's adoption of a relatively new design process. An appendix with a catalog of dynamic modulus values for frequently used mixes in Pakistan would be useful and serve as the foundation for the mechanistic-empirical pavement design guide structural method.

According to sensitivity analysis, mixtures with 6 percent SBS exhibit the greatest dynamic modulus values. The viscous component of an asphalt mixture is represented by a greater phase angle value, whilst the elastic behavior is represented by a lower phase angle

value. At higher and lower temperatures, the phase angle of a mixture containing 0% SBS is greater and tends to be viscous.

5.2 Conclusions

Based on the above consistency and performance testing, the following conclusions have been drawn from this research study:

a) When SBS content was raised to 7 percent, the modifier became the dominant matrix and formed an uninterrupted film around the droplets of the binder. This resulted in an increase in penetration value up to a critical concentration of 6 percent. Consequently, a dose of **6 percent SBS** is recommended since the penetration value stabilizes as the SBS percentage rises. Overall, a **46% drop** in penetration value is observed.

b) An increase in the proportion of SBS causes the softening point to rise. Bitumen's softening point rises as its asphaltene concentration rises, making it more viscous. Polymer swelling and maltene absorption by the polymer phase led to a rise in asphaltene concentration and a stiffer mix because of the softening point rising from 49°C to 80°C and overall, a **63% increase** in softening point was observed.

c) Ductility decreased from 100 to 64 and a **56% drop** is observed as due to the addition of SBS, the mix becomes stiffer and a reduction in bitumen ductility occurs as it becomes brittle, However, 50 ductility value is acceptable for road works, and in our case, 7% SBS is showing 64 value, therefore, 6% SBS content is suggested as optimal as it qualifies other testing specifications also.

d) Specimens with 6% SBS content were showing higher |E*| as compared to other mixes at frequencies 25, 10, 5, 1, 0.5 & 0.1 Hz on low and High temperatures. **An average increase in 2.10 times |E*|** was observed at **6% SBS** at different frequencies as compared to the unmodified mix which is also optimal SBS % recommended to use in the HMA mix.

e) Two-level factorial design analysis results showed that Temperature, Frequency, and SBS have a significant impact on |E*| and phase angle.

f) Phase angle initially increased with increasing temperature and then start decreasing after attaining a peak value at 37.8 ˚ C at lower frequencies. This was owing to asphalt concrete's reduced temperature dependence on the binder and greater temperature interaction with aggregate.

g) Master curves showed that higher E* was observed at **6% SBS** at lower and higher temperatures & frequencies. Hence **6% SBS** dosage by weight of binder is recommended for use in HMA at any temperature in Pakistan.

h) Statistical models were developed using Cobb-Douglas formulation incorporating temperature, frequency, and SBS as independent variables, The $\mathbf{R^2}$ for a model is **79%.**

i) Model validation by Multi Linear Programming (MEPX) shows the coefficient of determination R^2 is **0.966,** it means 96.6% variation in model is explained by response i.e., Dynamic Modulus |E*|

j) Isothermal and Isochronal plots revealed that the 0% SBS mix is showing an increase in Phase angle and less drop is observed due to higher bitumen content as compared to other mixes.

5.3 Recommendations

Study findings conclude that **6% of SBS content by the weight of bitumen** has outperformed as compared to other mixes. Because the mixture is stiffer, it has been shown to have lower penetration and ductility values and an increased softening point, making it more durable for HMA, or higher rust and fatigue resistant mix. Higher |E*| was observed at 6% SBS content, with an increase in |E*| value compared to the standard mix. As a result, the research suggests using bitumen with a 6 percent SBS concentration by weight in Pakistan's hotter and colder regions. Several further performance tests, such as the Flow number & Flow time, indirect tensile strength test, and Hamburg wheel tracker should be carried out to completely define the mixtures used in this research, however, for now, the study is mainly concerned with measuring dynamic modulus. To find out how resistant the material is to fatigue cracking, an indirect tension fatigue test should also be performed. Binder and aggregate combinations may be improved by examining the impacts of different binder and aggregate sources. Testing has been completed and it's time for the national level to embrace this challenge by implementing a performance-based design and analysis process that includes all stakeholders including contractors, consultants' clients, in Pakistan.

5.2 Contributions to State-of-the-Practice

A foundation for the deployment of a performance-based design system is provided by this research. The default dynamic modulus values discovered in this study were created

by master curve development, which will ultimately serve as the foundation for the adoption of a mechanistic-empirical design and analysis approach that is suitable for the Pakistan region where premature failure is frequently observed. It is also useful for enhancing the existing mix design, which is empirical since the dynamic modulus catalog at various temperatures and frequencies is supplied.

References

AASHTO, TP 62-07. (2007). *Standard Test Method for Determining the Dynamic Modulus of Hot Mix Asphalt (HMA)*. American Association of State Highway and Transportation Officials.

Airey, G. D. (2002). Road Materials and Pavement Design Use of Black Diagrams to Identify Inconsistencies in Rheological Data Use of Black Diagrams to Identify Inconsistencies in Rheological Data. *Road Materials and Pavement Design*, *3*(4), 403–424. http://www.tandfonline.com/doi/abs/10.1080/14680629.2002.9689933

Al-Hadidy, A. I., & Yi-qiu, T. (2009). Effect of polyethylene on life of flexible pavements. *Construction and Building Materials*, *23*(3), 1456–1464. https://doi.org/10.1016/j.conbuildmat.2008.07.004

Asphalt Institute MS-4. (1988). *The Asphalt Handbook (The Asphalt Institute,1988).pdf*. AsphaltInstitute.https://archive.org/details/TheAsphaltHandbookTheAsphaltInstitute1988

Al-Khateeb, G. G., & Ghuzlan, K. A. (2014). The combined effect of loading frequency, temperature, and stress level on the fatigue life of asphalt paving mixtures using the IDT test configuration. *International Journal of Fatigue*, *59*, 254–261. https://doi.org/10.1016/j.ijfatigue.2013.08.011

Baladi, G. Y., Haider, S. W., & Mirza, M. W. (2011). *Implementation of Superpave Binder and Asphalt Mix*. 1–23.

Bonnaure, F. G., Gravois, A., & Uge, P. (1977). *"A New Method for Predicting the Stiffness of Asphalt Paving Mixtures"*. Proceedings, Association of Asphalt Paving Technologists: Vol. 46, pp. 64-100.

Brule, B. (1999). The structure of polymer modified binders and corresponding asphalt mixtures. *Proceedings of the Association of Asphalt Paving Technologists*, *68*, 64–88.

Carpenter, S. H., Pine, W. J., & Trepanier, J. (2012). IMPACT OF HIGH RAP CONTENT ON STRUCTURAL AND PERFORMANCE Prepared By. *CIVIL ENGINEERING STUDIES Illinois Center for Transportation Series No. 12-002 UILU-ENG-2012-2006 ISSN: 0197-9191*, *12*.

Cross, S. A., & Jakatimath, Y. (2007). "*Determination of Dynamic Modulus Master Curves for Oklahoma HMA Mixtures"*. Oklahoma Department of Transportation: Final report.

Haghshenas, H., Nabizadeh, H., Kim, Y.-R., & Santosh, K. (2019). *Research on High-RAP Asphalt Mixtures with Rejuvenators and WMA Additives*. *September*, 66. http://digitalcommons.unl.edu/ndor

Kakade, V. B., Amaranatha Reddy, M., & Sudhakar Reddy, K. (2016). Effect of aging on fatigue performance of hydrated lime modified bituminous mixes. *Construction and Building Materials*, *113*, 1034–1043. https://doi.org/10.1016/j.conbuildmat.2016.03.066

Kalyoncuoglu, S. F., & Tigdemir, M. (2011). A model for dynamic creep evaluation of SBS modified HMA mixtures. *Construction and Building Materials*, *25*(2), 859–866. https://doi.org/10.1016/j.conbuildmat.2010.06.101

Kallas, B. F. (1970). "Dynamic Modulus of Asphalt Concrete in Tension and Tension-Compression". Proceedings, Association of Asphalt Paving Technologists: Vol. 39, pp. 1-20.

Khattab, A. M., El-Badawy, S. M., & Elmwafi, M. (2014). Evaluation of Witczak E* predictive models for the implementation of AASHTOWare-Pavement ME Design in the Kingdom of Saudi Arabia. *Construction and Building Materials*, *64*, 360–369.

Khodaii, A., & Mehrara, A. (2009). Evaluation of permanent deformation of unmodified and SBS modified asphalt mixtures using dynamic creep test. *Construction and Building Materials*, *23*(7), 2586–2592. https://doi.org/10.1016/j.conbuildmat.2009.02.015

Kim, Y., Park, H., Aragão, F., Building, J. L.-C. and, & 2009, undefined. (n.d.). Effects of aggregate structure on hot-mix asphalt rutting performance in low traffic volume local pavements. *Elsevier*. Retrieved July 19, 2022,

Miljkovic, M., & Radenberg, M. (2011). Rutting mechanisms and advanced laboratory testing of asphalt mixtures resistance against permanent deformation. *Facta Universitatis - Series: Architecture and Civil Engineering*, *9*(3), 407–417. https://doi.org/10.2298/fuace1103407m

Roque, R., Birgisson, B., Drakos, C., & Sholar, G. (2005). *Guidelines for use of modified binders*.

Tashman, L. and M. A. Elangovan. *Dynamic Modulus Test - Laboratory Investigationand Future Implementation in the State of Washington*. Washington State Department of Transportation Final Report. Final Research Report No. WA-RD 704.1, 2007

Witczak, M. W., and R. E. Root, "Summary of Complex Modulus Laboratory Test Procedures and Results," *STP 561*, American Society for Testing and Materials, 1974, pp. 67-94

Witczak, M.W., K. Kaloush, T. Pellinen, and M. El-Basyouny. *Simple Performance Test for Superpave Mix Design*. National Cooperative Highway Research Program (NCHRP) Report 465, Transportation Research Board, National Research Council, Washington, D.C., 2002.

Xu, T., & Huang, X. (2012). Investigation into causes of in-place rutting in asphalt pavement. *Construction and Building Materials*, *28*(1), 525–530. https://doi.org/10.1016/j.conbuildmat.2011.09.007

Yang, Z., Peng, H., Wang, W., & Liu, T. (2010). Crystallization behavior of poly(ε-caprolactone)/layered double hydroxide nanocomposites. *Journal of Applied Polymer Science*, *116*(5), 2658–2667. https://doi.org/10.1002/app

Zhang, C., Wang, H., You, Z., Gao, J., & Irfan, M. (2019). Performance test on Styrene-Butadiene-Styrene (SBS) modified asphalt based on the different evaluation methods. *Applied Sciences (Switzerland)*, *9*(3), 1–11. https://doi.org/10.3390/app9030467

Zhu, T., Ma, T., Huang, X., & Wang, S. (2016). Evaluating the rutting resistance of asphalt mixtures using a simplified triaxial repeated load test. *Construction and Building Materials*, *116*, 72–78. https://doi.org/10.1016/j.conbuildmat.2016.04.102

Zhang, W., Drescher, A., and D. E. Newcomb, Viscoelastic Behavior of Asphalt Concrete in Diametral Compression," *Journal of Transportation Engineering*, November/December 1997, pp. 495-502.

APPENDICES

APPENDIX A

DYNAMIC MODULUS |E*| TEST RESULTS

Table 1: Dynamic Modulus Test Results for 0% SBS Mix

Temperature (Celsius)	Frequency (Hz)	Dynamic Modulus (MPa)				SD	COV (%)
		Specimen 1	Specimen 2	Specimen 3	Mean		
4.4	25	18836	19034	18569	18813	233.351	1.24
	10	17523	17583	17320	17475.3	137.83	0.79
	5	16522	16433	16236	16397	146.36	0.89
	1	13580	13599	13491	13556.7	57.66	0.43
	0.5	12329	12303	12236	12289.3	47.98	0.39
	0.1	9283	9392	9365	9346.7	56.77	0.61
21.1	25	8086	8575	8870	8510.3	395.98	4.65
	10	6726	6984	7178	6962.7	226.75	3.26
	5	5641	5887	6086	5871.3	222.91	3.80
	1	3589	3701	3838	3709.3	124.71	3.36
	0.5	2919	2969	3071	2986.3	77.47	2.59
	0.1	1682	1705	1664	1683.7	20.55	1.22
37.8	25	4255	4121	3977	4117.7	139.03	3.38
	10	2882	3167	3032	3027	142.57	4.71
	5	2336	2192	2459	2329	133.64	5.74
	1	1202	1280	1118	1200	81.02	6.75
	0.5	885.6	953.3	826.9	888.6	63.25	7.12
	0.1	458.9	437.9	487.1	461.3	24.69	5.35
	0.01	309.8	298.4	184.3	264.2	69.40	26.27
54.4	25	1025	1011	942.7	992.9	44.03	4.43
	10	663.6	666.8	624.3	651.6	23.67	3.63
	5	482.7	483.2	456.4	474.1	15.33	3.23
	1	262.6	249.3	264.7	258.9	8.35	3.23
	0.5	215.4	203.3	212.9	210.5	6.39	3.03
	0.1	151.5	150.8	147.1	149.8	2.36	1.58

Table 2: Dynamic Modulus Test Results for 2% SBS Mix

Temperature (Celsius)	Frequency (Hz)	Dynamic Modulus (MPa)				SD	COV (%)
		Specimen 1	Specimen 2	Specimen 3	Mean		
4.4	25	23783	23967	23546	23765.3	211.06	0.89
	10	22729	22531	21853	22371	459.40	2.05
	5	20341	21460	21214	21005	588.05	2.80
	1	16960	18728	17683	17990.3	888.87	5.00
	0.5	15400	17375	16995	16590	1047.94	6.32
	0.1	11884	13841	13412	13045.7	1028.65	7.88
21.1	25	10349	10951	10736	10678.	305.07	2.86
	10	8628	9099	9051	8926.0	259.19	2.90
	5	7463	7763	7849	7691.7	202.65	2.63
	1	5009	5109	5263	5127.0	127.95	2.50
	0.5	4134	4166	4374	4224.7	130.31	3.08
	0.1	2479	2419	2550	2482.7	65.58	2.64
37.8	25	4455	4801	4293	4516.3	259.49	5.75
	10	3196	3473	3048	3239.0	215.74	6.66
	5	2414	2627	2263	2434.7	182.88	7.51
	1	1191	1316	1099	1202.0	108.92	9.06
	0.5	869.8	965	795.5	876.8	84.96	9.69
	0.1	446.9	490.5	424.3	453.9	33.65	7.41
	0.01	305.6	334.8	284.4	308.3	25.31	8.21
54.4	25	1624	1661	1684	1656.3	30.27	1.83
	10	1132	1174	1181	1162.3	26.50	2.28
	5	854.8	891.2	890.4	878.8	20.79	2.37
	1	474.3	474.7	482	477.0	4.33	0.91
	0.5	381.7	383.3	385.6	383.5	1.96	0.51
	0.1	255.3	244.7	252.5	250.8	5.49	2.19

Table 3: Dynamic Modulus Test Results for 3% SBS Mix

Temperature (Celsius)	Frequency (Hz)	Dynamic Modulus (MPa)				SD	COV (%)
		Specimen 1	Specimen 2	Specimen 3	Mean		
4.4	25	23884	24050	24297	24077	207.82	0.86
	10	22052	22304	23023	22459	503.87	2.24
	5	20643	20832	22015	21163	743.59	3.51
	1	17163	17321	19396	17960	1246.1	6.94
	0.5	15609	15812	18136	16519	1404.0	8.50
	0.1	11985	12167	14613	12921	1467.5	11.36
21.1	25	11155	11206	11240	11200	42.78	0.38
	10	9331	9562	9559	9484.0	132.51	1.40
	5	8028	8272	8398	8232.7	188.11	2.28
	1	5244	5526	5663	5477.7	213.64	3.90
	0.5	4206	4559	4649	4471.3	234.15	5.24
	0.1	2316	2633	2697	2548.7	204.02	8.00
37.8	25	6847	7278	6459	6861.3	409.69	5.97
	10	5427	5591	5086	5368.0	257.62	4.80
	5	4536	4516	4193	4415.0	192.52	4.36
	1	2772	2537	2486	2598.3	152.55	5.87
	0.5	2199	1895	1943	2012.3	163.43	8.12
	0.1	1142	978.7	1004	1041.6	87.89	8.44
	0.01	834.6	712.6	556	701.1	139.66	19.92
54.4	25	1717	2000	2406	2041.0	346.32	16.97
	10	1083	1306	1590	1326.3	254.11	19.16
	5	773.5	939.9	1170	961.1	199.10	20.72
	1	388.7	468.3	620.3	492.4	117.67	23.90
	0.5	296.6	345.9	485	375.8	97.70	26.00
	0.1	176.1	192.9	312.6	227.2	74.43	32.76

Table 4: Dynamic Modulus Test Results for 4% SBS Mix

Temperature (Celsius)	Frequency (Hz)	Dynamic Modulus (MPa)				SD	COV (%)
		Specimen 1	Specimen 2	Specimen 3	Mean		
4.4	25	24211	24985	24466	24554.0	394.43	1.61
	10	23141	23210	22630	22993.7	316.83	1.38
	5	22821	22112	21291	22074.7	765.68	3.47
	1	20233	18875	18238	19115.3	1018.98	5.33
	0.5	18785	17337	16759	17627.0	1043.67	5.92
	0.1	14485	13754	13234	13824.3	628.46	4.55
21.1	25	11554	11715	11319	11529.3	199.15	1.73
	10	9819	9763	9476	9686.0	184.01	1.90
	5	8649	8367	8190	8402.0	231.49	2.76
	1	6111	5517	5413	5680.3	376.58	6.63
	0.5	5162	4567	4384	4704.3	406.78	8.65
	0.1	3238	2765	2460	2821.0	392.01	13.90
37.8	25	8285	8472	7933	8230.0	273.68	3.33
	10	6516	6639	6263	6472.7	191.71	2.96
	5	5314	5429	5158	5300.3	136.02	2.57
	1	3035	3103	3005	3047.7	50.21	1.65
	0.5	2306	2321	2266	2297.7	28.43	1.24
	0.1	1205	1097	1149	1150.3	54.01	4.70
	0.01	971.5	785.4	601	786.0	185.25	23.57
54.4	25	2766	3386	3444	3198.7	375.82	11.75
	10	1880	2355	2440	2225.0	301.79	13.56
	5	1392	1753	1836	1660.3	236.06	14.22
	1	720.8	917	939.5	859.1	120.30	14.00
	0.5	553.6	718.8	708.3	660.2	92.50	14.01
	0.1	336.4	449.8	392.2	392.8	56.70	14.44

Table 5: Dynamic Modulus Test Results for 5% SBS Mix

Temperature (Celsius)	Frequency (Hz)	Dynamic Modulus (MPa)				SD	COV (%)
		Specimen 1	Specimen 2	Specimen 3	Mean		
4.4	25	26055	26518	26253	26275.3	232.31	0.88
	10	24147	24757	24685	24529.7	333.35	1.36
	5	22613	23116	23520	23083.0	454.40	1.97
	1	18902	19208	20784	19631.3	1009.90	5.14
	0.5	17312	17436	19451	18066.3	1200.76	6.65
	0.1	13205	13432	15879	14172.0	1482.66	10.46
21.1	25	13339	13953	11812	13034.7	1102.47	8.46
	10	10673	11852	10118	10881.0	885.52	8.14
	5	9326	10414	8895	9545.0	782.82	8.20
	1	6486	7043	6337	6622.0	372.13	5.62
	0.5	5468	5822	5353	5547.7	244.44	4.41
	0.1	3505	3417	3368	3430.0	69.42	2.02
37.8	25	8826	9302	8472	8866.7	416.49	4.70
	10	7092	7513	6639	7081.3	437.10	6.17
	5	5946	6154	5429	5843.0	373.31	6.39
	1	3628	3662	3103	3464.3	313.39	9.05
	0.5	2792	2818	2321	2643.7	279.74	10.58
	0.1	1401	1337	1097	1278.3	160.27	12.54
	0.01	1012	985.4	482	826.5	298.61	36.13
54.4	25	3991	4117	3662	3923.3	234.93	5.99
	10	2837	2840	2918	2865.0	45.92	1.60
	5	2129	2129	2298	2185.3	97.57	4.46
	1	1092	1097	990	1059.7	60.38	5.70
	0.5	845	835.5	839	839.8	4.80	0.57
	0.1	494.7	488.5	504	495.7	7.80	1.57

Table 6: Dynamic Modulus Test Results for 6% SBS Mix

Temperature (Celsius)	Frequency (Hz)	Dynamic Modulus (MPa)				SD	COV (%)
		Specimen 1	Specimen 2	Specimen 3	Mean		
4.4	25	28925	29012	31250	29729.0	1317.94	4.43
	10	27409	26564	30066	28013.0	1827.46	6.52
	5	26310	24649	28939	26632.7	2163.13	8.12
	1	23070	20590	25863	23174.3	2638.05	11.38
	0.5	26163	18451	24545	23053.0	4066.73	17.64
	0.1	28005	14258	21101	21121.3	6873.52	32.54
21.1	25	16256	16511	16964	16577.0	358.58	2.16
	10	13791	14049	14493	14111.0	355.08	2.52
	5	12102	12323	12702	12375.7	303.45	2.45
	1	8228	8437	8735	8466.7	254.80	3.01
	0.5	6709	6911	7152	6924.0	221.79	3.20
	0.1	3758	3923	4143	3941.3	193.15	4.90
37.8	25	10270	11061	14091	11807.3	2016.87	17.08
	10	8503	8599	11647	9583.0	1788.12	18.66
	5	7219	6594	9900	7904.3	1756.32	22.22
	1	4543	3906	6187	4878.7	1176.96	24.12
	0.5	3548	2857	4739	3714.7	952.01	25.63
	0.1	1800	1326	2216	1780.7	445.31	25.01
	0.01	1710	1685	1034	1476.3	383.28	25.96
54.4	25	6832	7408	9561	7933.7	1438.44	18.13
	10	4826	5791	7261	5959.3	1226.20	20.58
	5	3596	4685	5673	4651.3	1038.91	22.34
	1	1739	2648	2959	2448.7	633.96	25.89
	0.5	1230	1934	2038	1734.0	439.56	25.35
	0.1	632.9	873.8	867.3	791.3	137.25	17.34

Table 7: Dynamic Modulus Test Results for 7% SBS Mix

Temperature (Celsius)	Frequency (Hz)	Dynamic Modulus (MPa)				SD	COV (%)
		Specimen 1	Specimen 2	Specimen 3	Mean		
4.4	25	27471	27331	26796	27199.3	356.24	1.31
	10	25785	25577	25008	25456.7	402.23	1.58
	5	24430	24055	23492	23992.3	472.13	1.97
	1	20878	20395	19728	20333.7	577.45	2.84
	0.5	19149	18630	17878	18552.3	639.05	3.44
	0.1	15018	14519	13735	14424.0	646.75	4.48
21.1	25	14102	15352	11505	13653.0	1962.4	14.37
	10	12050	12715	9439	11401.3	1731.6	15.19
	5	10576	10930	8008	9838.0	1594.6	16.21
	1	7360	7561	5265	6728.7	1271.5	18.90
	0.5	6139	6343	4253	5578.3	1152.3	20.66
	0.1	3658	3839	2504	3333.7	724.19	21.72
37.8	25	9515	9709	7933	9052.3	974.21	10.76
	10	7710	7401	6263	7124.7	762.05	10.70
	5	6516	5882	5158	5852.0	679.50	11.61
	1	3973	3145	3005	3374.3	523.16	15.50
	0.5	3052	2267	2266	2528.3	453.51	17.94
	0.1	1509	1094	1149	1250.7	225.41	18.02
	0.01	1380	815	431	875.3	477.37	54.54
54.4	25	4774	5487	4963	5074.7	369.38	7.28
	10	3514	4042	3752	3769.3	264.43	7.02
	5	2688	3132	2858	2892.7	224.02	7.74
	1	1373	1632	1492	1499.0	129.64	8.65
	0.5	1034	1186	1101	1107.0	76.18	6.88
	0.1	555.3	603.1	587	581.8	24.32	4.18

APPENDIX B

PHASE ANGLE RESULTS

TABLE A-1: Phase Angle Results for 0% SBS Mix

Temperature (Celsius)	Frequency (Hz)	Phase Angle (Degrees)				SD	COV (%)
		Specimen 1	Specimen 2	Specimen 3	Mean		
4.4	25	8.69	8.7	8.5	8.6	0.11	1.31
	10	9.63	10.03	9.51	9.7	0.27	2.80
	5	10.98	11.17	10.56	10.9	0.31	2.86
	1	13.92	14.31	13.47	13.9	0.42	3.02
	0.5	15.3	15.51	14.9	15.2	0.31	2.03
	0.1	19.24	19.29	19.14	19.2	0.08	0.40
21.1	25	21.52	20.82	20.12	20.8	0.70	3.36
	10	25.01	23.66	23.21	24.0	0.94	3.91
	5	26.19	24.8	24.36	25.1	0.96	3.80
	1	28.95	27.46	27.1	27.8	0.98	3.52
	0.5	29.39	28.17	27.82	28.5	0.82	2.90
	0.1	30.65	30.18	30.12	30.3	0.29	0.96
37.8	25	29.04	29.03	29.19	29.1	0.09	0.31
	10	30.7	30.1	29.5	30.1	0.60	1.99
	5	30.33	30.5	30.51	30.4	0.10	0.33
	1	31.15	31.85	31.51	31.5	0.35	1.11
	0.5	32	32.1	32.19	32.1	0.10	0.30
	0.1	31.95	31.81	31.89	31.9	0.07	0.22
	0.01	30.67	31.09	31.53	31.1	0.43	1.38
54.4	25	32.2	31.54	32.02	31.9	0.34	1.07
	10	32.51	32.65	32.37	32.5	0.14	0.43
	5	31.71	31.32	31.19	31.4	0.27	0.86
	1	30.81	30.52	30.47	30.6	0.18	0.60
	0.5	29.91	29.75	29.45	29.7	0.23	0.79
	0.1	28.75	29	28.19	28.6	0.41	1.45

TABLE A-2: Phase Angle Results for 2% SBS Mix

Temperature (Celsius)	Frequency (Hz)	Phase Angle (Degrees)				SD	COV (%)
		Specimen 1	Specimen 2	Specimen 3	Mean		
4.4	25	8.27	8.76	7.43	8.2	0.67	8.25
	10	9.27	9.95	8.45	9.2	0.75	8.14
	5	10.12	10.16	9.19	9.8	0.55	5.59
	1	12.72	12.49	12.15	12.5	0.29	2.30
	0.5	13.6	13.79	13.35	13.6	0.22	1.63
	0.1	17.92	18.01	18.05	18.0	0.07	0.37
21.1	25	19.76	19.18	19.55	19.5	0.29	1.51
	10	23.35	22.39	23.52	23.1	0.61	2.64
	5	24.08	23.58	24.05	23.9	0.28	1.17
	1	26.83	25.59	25.6	26.0	0.71	2.74
	0.5	27.85	26.48	26.73	27.0	0.73	2.70
	0.1	30	28.36	29.18	29.2	0.82	2.81
37.8	25	28.81	28.92	29	28.9	0.10	0.33
	10	30.1	30.2	29.91	30.1	0.15	0.49
	5	30.9	29.5	30.85	30.4	0.79	2.61
	1	31.5	30.65	31.59	31.2	0.52	1.66
	0.5	29.12	29.19	29.2	29.2	0.04	0.15
	0.1	28.91	29.1	29.05	29.0	0.10	0.34
	0.01	28.12	29.21	29.11	28.8	0.60	2.09
54.4	25	29.55	29.75	29.91	29.7	0.18	0.61
	10	30.41	30.49	30.62	30.5	0.11	0.35
	5	29.12	29.91	29.06	29.4	0.47	1.62
	1	28.91	28.79	28.61	28.8	0.15	0.52
	0.5	27.13	27.51	27.19	27.3	0.20	0.75
	0.1	28	28.2	27.92	28.0	0.14	0.51

TABLE A-3: Phase Angle Results for 3% SBS Mix

Temperature (Celsius)	Frequency (Hz)	Phase Angle (Degrees)				SD	COV (%)
		Specimen 1	Specimen 2	Specimen 3	Mean		
4.4	25	7.64	7.33	7.91	7.6	0.29	3.81
	10	9.16	9.2	6.54	8.3	1.52	18.37
	5	10.04	10.11	7.25	9.1	1.63	17.86
	1	12.54	12.19	9.4	11.4	1.72	15.13
	0.5	13.49	13.42	12.4	13.1	0.61	4.66
	0.1	17.14	17.06	16.71	17.0	0.23	1.35
21.1	25	18.71	18.52	18.25	18.5	0.23	1.25
	10	21.23	20.96	21.32	21.2	0.19	0.88
	5	22.64	22.82	21.6	22.4	0.66	2.95
	1	26.49	27.52	25.07	26.4	1.23	4.67
	0.5	27.71	28.61	26.17	27.5	1.23	4.49
	0.1	28.44	28.23	28.85	28.5	0.32	1.11
37.8	25	27.94	28.1	28.8	28.3	0.46	1.62
	10	28.87	28.97	29.56	29.1	0.37	1.28
	5	30	29.62	29.72	29.8	0.20	0.66
	1	30.22	30.48	30.18	30.3	0.16	0.54
	0.5	28.01	28.09	27.91	28.0	0.09	0.32
	0.1	27.8	27.65	27.85	27.8	0.10	0.37
	0.01	26.45	26.1	29.1	27.2	1.64	6.03
54.4	25	29.14	29.74	29.57	29.5	0.31	1.05
	10	30.05	30.14	30.19	30.1	0.07	0.24
	5	28.91	28.81	29.1	28.9	0.15	0.51
	1	27.15	27.21	27.03	27.1	0.09	0.34
	0.5	25.69	25.62	25.19	25.5	0.27	1.06
	0.1	24.01	24.41	24.19	24.2	0.20	0.83

TABLE A-4:Phase Angle Results for 4% SBS Mix

Temperature (Celsius)	Frequency (Hz)	Phase Angle (Degrees)				SD	COV (%)
		Specimen 1	Specimen 2	Specimen 3	Mean		
4.4	25	7.19	6.85	7.29	7.1	0.23	3.24
	10	7.75	7.51	8.32	7.9	0.42	5.29
	5	8.25	8.52	8.96	8.6	0.36	4.18
	1	6.99	10.68	10.75	9.5	2.15	22.70
	0.5	10.95	11.61	11.76	11.4	0.43	3.77
	0.1	15.24	15.79	14.29	15.1	0.76	5.02
21.1	25	16.42	18.82	18.01	17.8	1.22	6.88
	10	18.32	21.67	20.68	20.2	1.72	8.51
	5	19.19	23.44	22.35	21.7	2.21	10.19
	1	22.2	27.32	26.38	25.3	2.73	10.77
	0.5	23.2	28.05	27.62	26.3	2.68	10.21
	0.1	26.23	29.59	28.35	28.1	1.70	6.06
37.8	25	28.75	28.71	28.35	28.6	0.22	0.77
	10	28.15	28.94	29.31	28.8	0.59	2.06
	5	29.15	29.12	29.37	29.2	0.14	0.47
	1	30.09	30.11	30.07	30.1	0.02	0.07
	0.5	27.91	27.81	27.51	27.7	0.21	0.75
	0.1	27.12	27.16	26.85	27.0	0.17	0.62
	0.01	27.01	26.91	26.51	26.8	0.26	0.99
54.4	25	28	27.74	27.37	27.7	0.32	1.14
	10	29.26	29.13	29.67	29.4	0.28	0.96
	5	28.26	28.71	28	28.3	0.36	1.27
	1	26.65	26.64	26.71	26.7	0.04	0.14
	0.5	24.95	24.92	24.73	24.9	0.12	0.48
	0.1	24.1	23.91	23.51	23.8	0.30	1.26

TABLE A-5:Phase Angle Results for 5% SBS Mix

Temperature (Celsius)	Frequency (Hz)	Phase Angle (Degrees)				SD	COV (%)
		Specimen 1	Specimen 2	Specimen 3	Mean		
4.4	25	6.92	6.71	6.25	6.6	0.34	5.17
	10	9.31	8.8	6.1	8.1	1.73	21.38
	5	10.3	9.73	6.58	8.9	2.00	22.59
	1	9.12	9.42	9.4	9.3	0.17	1.80
	0.5	10.19	11.4	10.15	10.6	0.71	6.71
	0.1	15.11	14.94	14.39	14.8	0.38	2.54
21.1	25	16.23	16.76	15.94	16.3	0.42	2.55
	10	17.3	19.15	17.76	18.1	0.96	5.33
	5	18.68	20.38	18.82	19.3	0.94	4.89
	1	22.69	23.43	22.08	22.7	0.68	2.97
	0.5	23.78	25.66	23.18	24.2	1.29	5.35
	0.1	26.77	28.77	26.27	27.3	1.32	4.85
37.8	25	28.13	27.17	27.44	27.6	0.50	1.80
	10	28.14	28.22	28.35	28.2	0.11	0.38
	5	28.41	28.77	28.28	28.5	0.25	0.89
	1	29.69	29.31	29	29.3	0.35	1.18
	0.5	27.32	27.11	27.07	27.2	0.13	0.49
	0.1	26.62	26.51	26.4	26.5	0.11	0.41
	0.01	26.14	26.12	25.87	26.0	0.15	0.58
54.4	25	27.96	27.57	27.1	27.5	0.43	1.56
	10	28.77	28.82	28.42	28.7	0.22	0.76
	5	27.92	27.89	27.14	27.7	0.44	1.60
	1	26.51	26.37	26.66	26.5	0.15	0.55
	0.5	24.07	23.57	23.77	23.8	0.25	1.06
	0.1	22.58	22.91	22.81	22.8	0.17	0.74

TABLE A-6:Phase Angle Results for 6% SBS Mix

Temperature (Celsius)	Frequency (Hz)	Phase Angle (Degrees)				SD	COV (%)
		Specimen 1	Specimen 2	Specimen 3	Mean		
4.4	25	6.15	6.12	5.97	6.1	0.10	1.59
	10	7.22	7.99	7.25	7.5	0.44	5.83
	5	7.81	9.22	7.67	8.2	0.86	10.41
	1	9.42	9.32	9	9.2	0.22	2.37
	0.5	10.12	10.27	9.95	10.1	0.16	1.58
	0.1	14.14	14.76	14.29	14.4	0.32	2.25
21.1	25	16.14	16.25	16.31	16.2	0.09	0.53
	10	18.11	18.01	17.85	18.0	0.13	0.73
	5	19.23	19.2	19.07	19.2	0.09	0.44
	1	22.35	22.12	22.07	22.2	0.15	0.67
	0.5	23.91	23.99	24.09	24.0	0.09	0.38
	0.1	27.15	27.18	27.01	27.1	0.09	0.33
37.8	25	27.93	27.24	27.35	27.5	0.37	1.35
	10	27.71	27.81	27.67	27.7	0.07	0.26
	5	28.01	27.91	27.95	28.0	0.05	0.18
	1	28.88	29.44	28.35	28.9	0.55	1.89
	0.5	26.98	26.57	26.21	26.6	0.39	1.45
	0.1	25.5	25.48	25.64	25.5	0.09	0.34
	0.01	24.81	25.14	25.04	25.0	0.17	0.68
54.4	25	27.01	26.95	27.19	27.1	0.12	0.46
	10	28.48	28.51	28.32	28.4	0.10	0.36
	5	26.95	26.97	26.81	26.9	0.09	0.32
	1	25.83	25.59	25.49	25.6	0.17	0.68
	0.5	23.76	23.59	23.08	23.5	0.35	1.51
	0.1	22.51	22.32	22.1	22.3	0.21	0.92

TABLE A-7:Phase Angle Results for 7% SBS Mix

Temperature (Celsius)	Frequency (Hz)	Phase Angle (Degrees)				SD	COV (%)
		Specimen 1	Specimen 2	Specimen 3	Mean		
4.4	25	6.23	5.33	5.94	5.8	0.46	7.88
	10	7.21	7.28	7.44	7.3	0.12	1.61
	5	8.02	8.11	8.19	8.1	0.09	1.05
	1	8.65	8.54	8.55	8.6	0.06	0.71
	0.5	9.67	10.09	10.12	10.0	0.25	2.53
	0.1	13.93	14.22	13.97	14.0	0.16	1.12
21.1	25	15.41	15.33	15.43	15.4	0.05	0.34
	10	17.82	17.19	17.71	17.6	0.34	1.91
	5	18.86	18.19	19.05	18.7	0.45	2.42
	1	21.93	22.12	21.85	22.0	0.14	0.63
	0.5	23.45	23.81	23.69	23.7	0.18	0.78
	0.1	26.82	26.68	26.54	26.7	0.14	0.52
37.8	25	26.75	26.563	26.83	26.7	0.14	0.51
	10	27.39	27.27	27.22	27.3	0.09	0.32
	5	26.61	27.69	27.05	27.1	0.54	2.00
	1	28.39	28.07	28.16	28.2	0.17	0.59
	0.5	26.12	26.29	26.22	26.2	0.09	0.33
	0.1	25.31	25.22	25.19	25.2	0.06	0.25
	0.01	24.52	24.12	24.3	24.3	0.20	0.82
54.4	25	26.12	26.01	26.22	26.1	0.11	0.40
	10	27.81	27.01	27.12	27.3	0.43	1.59
	5	26.19	26.12	26.32	26.2	0.10	0.39
	1	25.04	25.51	25.32	25.3	0.24	0.93
	0.5	22.01	22.12	22.09	22.1	0.06	0.26
	0.1	21.71	21.66	21.12	21.5	0.33	1.52